Title: Temporal evolution of target representation, movement direction planning, and reach execution in occipital-parietal-frontal cortex: an fMRI study

Authors: David C. Cappadocia[1-4], Simona Monaco[5], Ying Chen[1-4], Gunnar Blohm[4,6,8], and J. Douglas Crawford[1-4,7-8*]

1. Centre for Vision Research, York University, Toronto, ON, Canada
2. School of Kinesiology and Health Science, York University, Toronto, ON, Canada
3. Neuroscience Graduate Diploma Program, York University, Toronto, ON, Canada
4. Canadian Action Perception Network (CAPNet)
5. Center for Mind/Brain Sciences, University of Trento, Trento, Italy
6. Centre for Neuroscience Studies, Queen's University, Kingston, ON, Canada
7. Departments of Biology and Psychology, York University, Toronto, ON, Canada
8. Brain in Action CREATE / IRTG Program, Toronto, ON, Canada

*Correspondence:

J.D. Crawford
York University
Centre for Vision Research
0009A Lassonde Building
4700 Keele Street
Toronto, ON, M3J 1P3, Canada
jdc@yorku.ca

Abstract

The cortical mechanisms for reach have been studied extensively, but the directionally selective mechanisms for target memory, movement planning, and execution have not been clearly differentiated in the human. Here, we used an event-related fMRI design that included a target memory delay, followed by a pro-anti reach instruction, a planning delay, and finally a go instruction for movement. This sequence yielded temporally separable preparatory responses that expanded from modest parieto-frontal activation during target memory to broad occipital-parietal-frontal activation during planning and execution. Using the pro-anti instruction to differentiate visual vs. motor selectivity during planning, we found that only one occipital area showed contralateral *visual* selectivity, whereas a broad constellation of occipital, parietal, and frontal areas showed contralateral *movement* selectivity. Temporal analysis of these areas through the entire memory-planning sequence revealed early visual selectivity in most areas, followed by motor selectivity in most areas, with *all* areas showing a stereotypical visuomotor transition. Cross-correlation of these spatial parameters through time revealed separate functional networks for visual input, motor output, and visuomotor transformation that spanned occipital, parietal, and frontal cortex. These results demonstrate that a highly distributed occipital-parietal-frontal reach network is involved in the transformation of retrospective sensory information into prospective motor plans.

Keywords: fMRI, visual memory, visuomotor transformations, movement planning, reach

Introduction

In order to effectively interact with the world, human beings take in sensory information and use it to produce meaningful actions. One of the most commonly studied cases of this is visually-guided reach-to-touch movements (E.g., ringing a doorbell or pushing the power button on a laptop computer). Often visual information is no longer available by the time one makes a movement, or gaze has been re-directed to another location by the time one initiates a movement (Henriques et al., 1998; Flanagan & Johansson, 2003). To perform such movements, the brain must retain information about the spatial location of the target in working memory, use this to form a motor plan, and then execute that motor plan to reach towards the goal. Neurophysiological studies in awake behaving non-human primates have shown a progression from visual-to-motor coding within and between neurons in the occipital-parietal-frontal cortical axis (Picard and Strick, 2001; Andersen and Buneo, 2002; Gail and Andersen, 2006; Cisek and Kalaska, 2010; Westendorff et al., 2010; Kravitz et al., 2011), and spatially-selective networks for memory, attention, and planning that span parietal and frontal cortex (Berman and Colby, 2009; Rawley and Constantinidis, 2009). However, human imaging studies have not clearly differentiated spatial selectivity for reach plans in the cerebral cortex from target representation and/or motor execution, or tracked visual vs. motor selectivity through the entire sequence of events leading up to reach execution.

Previous human neuroimaging studies investigating visual-to-motor (visuomotor) transformations have identified several key regions in the parietal-frontal reach planning network. In parietal cortex, both the midposterior intraparietal sulcus (mIPS) (DeSouza et al., 2000; Medendorp et al., 2003, 2005; Prado et al., 2005; Beurze et al., 2007,

2009, 2010; Fernandez-Ruiz, 2007; Tosoni et al., 2008; Filimon et al., 2009; Chen et al., 2014) and the superior parietal occipital cortex (SPOC) (Astafiev et al., 2003; Connolly et al., 2003; Prado et al., 2005; Fernandez-Ruiz et al., 2007; Tosoni et al., 2008; Beurze et al., 2009; Gallivan et al., 2009, 2011; Bernier and Grafton, 2010; Cavina-Pratesi et al., 2010; Monaco et al., 2011; Chen et al., 2014) show activation related to reach planning and execution. These areas encode this information with contralateral left–right topography (Beurze et al., 2007; Vesia et al., 2010; 2012). In frontal cortex, human dorsal premotor cortex (PMd) also encodes pointing and reaching (Connolly et al., 2000, 2007; Astafiev et al., 2003; Prado et al., 2005; Beurze et al., 2007, 2009, 2010; Bernier et al., 2010, 2012; Chen et al., 2014), as well as contralateral spatial selectivity (Beurze et al., 2007, 2009, 2010; Bernier et al., 2012; Chen et al. 2014).

An important question in vision-memory-motor transformations is whether spatial locations and reach plans are specified in visual or motor coordinates, i.e., whether sustained spatial activity codes retrospective sensory information or prospective motor plans (Curtis, 2006). One strategy scientists have used to study this question is dissociating the visual target from the motor goal. Some studies have used anti-reaching tasks, where subjects view a target and must perform a reach in the opposite direction (Connolly et al., 2000; Chen et al., 2014; Gertz and Fiehler, 2015). Using this type of paradigm, Chen et al. (2014) found contralateral visual coding in left occipital cortex during the target representation period and contralateral motor coding in parieto-frontal cortex during movement execution. In another study, contralateral motor coding was observed in the left precuneus during movement planning (Gertz and Fiehler, 2015). Fernandez-Ruiz et al. (2007) studied visual and motor coding using reversing

prisms, which reverse the visual input such that a leftward reach target appears to be in the right visual field. They found that most regions in the left posterior parietal cortex (PPC) encoded the visual direction of the goal during movement execution (with the exception of the angular gyrus, which encoded the movement direction).

What all of these imaging studies lacked, leading to the current study, was a clear separation between target memory, motor planning, and motor execution. Some fMRI studies isolated reach planning from execution, but slow BOLD dynamics did not allow a distinction between visual target memory from motor planning (Connolly et al., 2000; Fernandez-Ruiz et al. 2007; Beurze et al., 2007, 2009). In other studies, target memory was separated from motor planning, but did not distinguish planning from execution (Connolly et al., 2000; Chen et al., 2014). Based on these studies, one might predict that parieto-frontal cortex should show contralateral directional tuning for reach plans, especially in the hemisphere contralateral to the hand (Connolly et al., 2003; Fernandez-Ruiz, 2007; Bernier et al., 2012; Gertz and Fiehler, 2015). However, one cannot clearly differentiate this spatial tuning for planning from coding target direction (and/or motor execution signals), especially in occipital cortex that might show tuning for either visual direction or an imaginary goal. Further, one cannot track visual versus motor tuning through a separate sequence of visual memory, planning, and execution events, or use this information to construct functional networks of sensory, motor, and sensorimotor codes for reach.

The current study uses an event-related fMRI paradigm that explicitly separates three phases in time (reach target representation, motor planning, and motor execution), by introducing a pro-anti reach instruction between target memory and

planning phases, and a ‘go signal’ between planning and execution times. We used this paradigm in combination with a new way of spatially analyzing combined pro / anti-reach data, to investigate four questions: (1) which brain areas are differentially activated for target representation, reach movement planning, and reach movement execution, (2) which of these areas show visual vs. motor directional specificity during the planning phase, (3) at what point in the target-planning-execution coding sequence does a visual-motor transformation occur *within* the cortical areas involved in reach, and (4) how are these visual, motor, and visuomotor parameters temporally and spatially distributed through the cortical networks for reach in the human?

Methods

Participants

Twelve right-handed subjects (3 males, 9 females aged 20-36) were recruited from the York University community. All subjects had normal or corrected-to-normal vision and none of the subjects had any known neurological deficits. The York University Human Participants Review Sub-committee approved all techniques used in this study and all participants gave their informed consent prior to the experiment.

Experimental stimuli and apparatus

The experimental stimuli and apparatus were the same as the setup used in Chen et al. (2014). Visual stimuli consisted of optic fibers embedded into a custom-built board with adjustable tilt. The board was mounted atop a platform whose height was also adjustable (Fig. 1A). The platform was attached to the MRI scanner bed and placed over the abdomen of the subject. The height of the platform and tilt of the board were adjusted for each participant to ensure comfortable reaching movements. A translucent touchscreen (Keytec, 170 mm X 126 mm) was affixed on the board to record reach endpoints. An eye-tracking system (iView X) was used in conjunction with the MRI-compatible Avotec Silent Vision system (RE-5701) to record movements of the right eye during the experiment.

The head of the participant was slightly tilted (~20º) to allow direct viewing of the stimuli presented on the board (Fig. 1A). The board was approximately perpendicular to gaze approximately 60 cm from the eyes. The upper arm was strapped to the scanner bed to limit motion artifacts. Reaches were thus performed by movements of the right

forearm and hand. A button pad was placed on the left side of the participants' abdomen and served as both the starting point for each trial and as the response for the color report control task (see experimental paradigm and timing). Participants wore headphones to hear auditory instructions and cues. During each trial, subjects were in complete darkness with the exception of the visual stimuli, which were not bright enough to illuminate the workspace. The hand was never visible to the subject, even during reaching.

There were 3 types of visual stimuli presented by different colors: the fixation point in yellow, targets in green or red, and masks in white. All stimuli were presented horizontally on the touch screen, and had the same diameter of 3mm as the optic fibres. There was one central fixation location. Eight horizontal peripheral targets (4 on each side of the touchscreen) were used (Fig. 1B), and twenty "mask" LEDs were located above and below the target line (ten on each side with five above and five below the targets). The visual mask was used during the delay periods to control for visual afterimages. The distance between the eyes of the subject and the center of the touch screen was approximately 60cm. The target LEDs were located approximately 4°, 5°, 6° or 7° to the left or right of the fixation LED.

Experimental paradigm and timing

We used an event-related design, with each trial lasting 38 seconds (including an inter-trial interval of 12 seconds). The paradigm included 3 tasks: pro-reach, anti-reach, and colour report as a control (Fig. 1B). Each trial began with the presentation of the yellow

fixation LED (this was displayed for 24 seconds before the first trial in each run). Concurrently, subjects were given the auditory instruction “reach” or “color” to indicate the task they had to perform at the end of that trial. The important distinction between these two instructions is that while remembering the spatial location of the target LED was required for the reaching trials, this information could be ignored for the colour report trials. After 2 seconds, a green or red target LED was illuminated for 2 seconds, followed by an 8 second delay period (the target representation phase) during which the fixation LED and mask LEDs were illuminated. At the end of the delay, subjects were given one of 3 auditory instructions: “towards” (indicating a pro-reach trial), “opposite” (indicating an anti-reach trial), or “color” (indicating a color report trial), which took 2 seconds. The pro- or anti-reach instruction being given in the middle of the trial prevented subjects from forming their movement plan during the first delay period. The auditory instruction was followed by another 8 second delay period (the motor planning phase) during which the fixation LED and mask LEDs were illuminated. After the mask LEDs were turned off, subjects heard a beep that served as a go signal for subjects to reach-to-touch to: 1) the remembered location of the target in pro-reach trials, 2) the mirror location in the opposite hemifield in anti-reach trials, or 3) press the button once if the target LED was green or twice if it was red for the colour report trials (or vice versa, this was be counterbalanced across subjects). This is referred to as the motor execution phase. After touching the touchscreen for 2 seconds, subjects heard a beep that instructed them to return their right index finger to the starting position. The following trial started 12 seconds later.

Each functional run consisted of 12 trials presented in a random order (4 for each of the three tasks; 50% of targets presented in each hemifield for each task) and lasted about 8 minutes. For the purpose of analysis, target locations were collapsed together as "left" or "right". Subjects participated in 8 functional runs in one session. They were trained to perform the required tasks 1-2 days before imaging and practiced all tasks within the MRI scanner before scanning to ensure that they were comfortable with the task.

Behavioral recordings

Following the fMRI experiments, the eye position and reach endpoints were inspected. Eye movement errors were defined as trials where subjects were unable to maintain visual fixation from target presentation until touching the touchscreen. Reaching errors were defined as reaches to the direction opposite to the instructed reach goal. Trials with behavioral errors were excluded from further analysis (4.52% of trials).

To confirm accurate reaching, we performed a correlation analysis comparing horizontal target location to the horizontal reach endpoint for each subject. For pro-reach trials, across-subject means of the correlation coefficients (r) were r=0.843±0.03. For anti-reach trials, across-subject means of the correlation coefficients were r=0.836±0.04. We then applied Fischer's r-to-z transformation to individual subject's r values and performed one-way t-tests to compare subjects' z scores to 0. Both t-tests were significant ($P_{pro} < 0.001$, $P_{anti} < 0.001$), indicating accurate reaching.

Imaging parameters

The experiment was conducted at the Sherman Health Sciences Centre at York University with a 3-T whole-body MRI system (Siemens Magnetom TIM Trio). The posterior half of a 12-channel head coil (6 channels) was placed at the back of the head, with a 4-channel flex coil over the anterior part of the head (Figure 1B). The head was tilted ~20º to allow direct viewing of the stimuli the experimental trials.

Functional data was acquired using an EPI (echo-planar imaging) sequence (repetition time [TR] = 2000 ms; echo time [TE] = 30 ms; flip angle [FA] = 90º; field of view [FOV] = 192 mm X 192 mm, matrix size = 64 X 64 leading to an in-slice resolution of 3 mm X 3 mm; slice thickness = 3.5 mm, no gap; 36 transverse slices angled at ~25º covering the whole brain). Slices were collected in ascending and interleaved order. During each experimental session, a T1 –weighted anatomical reference volume was acquired using a MPRAGE sequence (TR = 1900 ms; TE = 2.52 ms; inversion time TI = 900 ms; FA = 90º; FOV = 256 mm X 256 mm X 192 mm, voxel size = 1 X 1 X 1 mm^3).

Preprocessing

All data was analyzed using Brain Voyager QX 2.2 (Brain Innovation). The first 2 volumes of each scan were discarded to avoid T1 saturation effects. For each run, slice scan time correction (cubic spline), temporal filtering (removing frequencies <2 cycles/run) and 3D motion correction (trilinear/sinc) were performed. The 3D motion correction was performed by aligning each volume of one run to the volume of the functional scan that was closest in time to the anatomical scan. 3 runs showing abrupt

head movement of 1mm or 1º were discarded. Functional runs were coregistered to the anatomical image. Functional data was then transformed into Talairach space using the spatial transformation parameters from each individual subject's anatomical scan. The voxel size of the native functional images was 3x3x3 and was not resampled to a different voxel size during the preprocessing steps. Functional data was spatially smoothed using a FWHM of 8 mm.

Data analysis

For each participant, we used a general linear model with 34 predictors. Two predictors were used for the initial auditory instruction (reach or color); four predictors were used for target presentation (left or right X reach or color trial); four predictors were used for target representation (left or right X reach or color trial); six predictors were used for the 2^{nd} auditory instruction (left or right X pro-reach, anti-reach, or color trial); six predictors were used for motor preparation (left or right X pro-reach, anti-reach, or color trial); six predictors were used for motor execution (left or right X pro-reach, anti-reach, or color trial). In addition, six motion correction parameters and behavioral errors were added as confound errors. Each predictor was derived from a rectangular wave function convolved with a standard hemodynamic response function using Brain Voyager QX's default double-gamma hemodynamic response function.

Voxelwise analysis

Contrasts were performed on β weights using an RFX (random effects) GLM with a percentage signal change transformation. This GLM was used to investigate the two main questions for this study. To investigate the brain areas involved in spatial target representation, reach movement planning, and reach movement execution, we performed three contrasts to find brain areas that showed higher activity for reach trials (pro and anti) than the control (color) trials during each phase.

We also performed two contrasts to test if brain areas showed directionally selective activation in visual or motor coordinates during movement planning (see Figure 6). The first contrast was designed to find contralateral visually selective brain areas. For the left hemisphere, these areas showed higher activation when the target was initially presented in the right visual field (pro and anti right) than the left (pro and anti left). The other contrast aimed at finding movement-direction selective brain areas. For the left hemisphere, these areas showed higher activation when the movement direction was to the right (pro right and anti left) than the left (pro left and anti right. For these contrasts, we limited our analysis to brain regions showing higher BOLD activation in the hemisphere contralateral to the visual target or motor goal, respectively. These contrasts were performed on both hemispheres.

Activation maps for group voxelwise results were overlaid on the inflated brain of one representative subject. To correct for multiple comparisons, at the first stage of the analyses we applied a cluster threshold correction (Forman et al. 1995) using Brain Voyager's cluster-level statistical threshold estimator plug-in (Goebel et al. 2006) to the activation map resulting from each of the individual contrasts. This algorithm uses Monte Carlo simulations (1,000 iterations) to estimate the probability of a number of

contiguous voxels being active purely due to chance while taking into consideration the average smoothness of the statistical maps. This approach allows the rigor of correction for multiple comparisons to reduce type I errors while also identifying areas that may be vulnerable to type II errors, which often go unacknowledged (Lieberman and Cunningham 2009). We only showed results for areas that survived cluster threshold correction. At the second stage of the analyses, we applied Bonferroni correction to the comparisons between the beta weights extracted from each area. In particular, we corrected our p-value for the two types of contrasts that were performed in this task aimed at answering different questions ($p<0.05/2 = p<0.025$). A Bonferroni correction was also applied to the t value for each contrast to account for the two main contrast types we performed on this data set (movement trials > control trials and directional selectivity)

a cluster threshold correction (Forman et al., 1995) was performed using brain voyager QX's cluster-level statistical threshold estimator plug-in (1000 iterations). Areas that did not survive were excluded from further analysis. A Bonferroni correction was also applied to the *t* value for each contrast to account for the two main contrast types we preformed on this data set (movement trials > control trials and directional selectivity; $\alpha = 0.5 / 2$ comparisons $= 0.025$ corrected for $p < 0.05$).

Results

General Reach Activation: Target Memory vs. Motor Planning vs. Motor Execution

In our first analysis, we looked at general, non-directional reach activation; combining left and right movements for both pro and anti-reach trials (a recent fMRI study has shown that pro and anti-reaches activate similar parietal and premotor areas; Gertz and Fiehler, 2015). Figure 2A, B, and C plots these data relative to our control task in each of the three major phases of our task: target representation, motor planning, and motor execution, with corresponding ß-weights for these data shown in supplementary Figure 1, and the corresponding Talairach coordinates shown in Tables 1, 2, and 3. We also provided complete time series data for select areas (Figure 3). These data are described in more detail in the following sections.

Task related activation during the target representation phase: Contrast 1 [Target Representation Reach > Target Representation Color] investigated which brain areas showed higher activation for spatial coding required to plan a reach (either pro or anti) than activation related to representing the color of the target (the requirement of the control task). In this phase, only the visual target location was known (as reach

direction was only specified by an auditory instruction after this delay period), and any activation revealed by this contrast may be related to any aspect of target coding (not necessarily direction). Figure 2A shows the activation map for this contrast superimposed on inflated cortical surfaces viewed from above. The indicated areas survived a cluster threshold correction of 82 voxels. This contrast revealed a rather modest amount of activation in bilateral dorsal premotor cortex (PMd, near BA 6) and the right posterior intraparietal sulcus (pIPS). At first glance it might seem odd that only areas associated with movement control (Gallivan and Culham, 2015) were activated, but recall that the control task also involves memory, of a non-spatial, non-motor target type. Thus, this subtraction shows areas with memory-epoch activity *specific to spatial location or reach*.

Task related activation during the motor preparation phase: Contrast 2 [Motor Preparation Reach (pro + anti) > Motor Preparation Color] investigated which brain areas showed higher activation for the motor planning required to plan a pro or anti-reach than activation related to representing the color of the target (the requirement of the control task). Activation during this phase could be related to planning a specific movement and/or general motor preparation in anticipation of an upcoming reach. The activation map for this contrast is shown on an inflated cortical surface viewed from the lateral and medial sides (Figure 2b). The marked areas survived a cluster threshold correction of 230 voxels. This contrast revealed widespread activation in bilateral dorsal premotor cortex (PMd, near BA 6), ventral premotor cortex (PMv), supplementary motor area (SMA), cingulate motor area (CMA), midposterior intraparietal sulcus (mIPS), posterior intraparietal sulcus (pIPS), superior occipital gyrus (SOG), lingual

gyrus (LG). Activation was also found in the left hemisphere in primary motor cortex (M1), superior parietal occipital cortex (SPOC), and inferior occipital gyrus (IOG), and in right primary somatosensory cortex (S1).

Task related activation during the motor execution phase: Contrast 3 [Motor Execution Reach (pro + anti) > Motor Execution Color] investigated which brain areas showed higher activation related to executing a pro or anti-reach than activation related to indicating the color of the target with a button press (the requirement of the control task). The activation map for this contrast is shown on an inflated cortical surface (Figure 2C). The marked areas survived a cluster threshold correction of 206 voxels. This contrast revealed widespread activation in bilateral mIPS, M1, PMd (near BA 6), inferior frontal gyrus (IFG), supramarginal gyrus (SMG), and IOG. Activation was also found in the left hemisphere in primary somatosensory cortex (S1), in the right hemisphere in the middle frontal gyrus (MFG), and in the supplementary motor area (SMA) (could not disentangle the right and left hemisphere for SMA).

Time series data: To better understand the evolution of activation for these brain areas, we examined their time series. Figure 3 illustrates the time courses data of the reach and color conditions for 4 representative bilateral brain areas, chosen because they have been linked to visuomotor planning, including: superior occipital gyrus (SOG), posterior intraparietal sulcus (pIPS), midposterior intraparietal sulcus (mIPS), and dorsal premotor cortex (PMd). We selected these areas as SOG showed egocentric planning-related activation in a previous study (Chen et al., 2014) and pIPS, mIPS, and PMd are part of the parieto-frontal reach planning network (Culham et al., 2006; Gallivan et al., 2011, Vesia et al., 2012). The onset time for target representation, movement planning,

and movement execution are indicated by grey vertical lines (noting that the BOLD response data have been time-corrected for estimated hemodynamic lag), with black lines indicating peak values during these 3 phases from left to right, respectively.

Looking at these representative time courses, several patterns emerge that help to understand the previous observations and provide reference events for further analysis. First, in nearly all of our regions of interests three peaks of activation were apparent, aligned closely with target representation, movement planning, and motor execution. An exception to this general trend was the lack of a distinctive third execution peak for some occipital areas, such as left SOG (Figure 3) and bilateral LG (not shown). Second, the relative heights of these peaks were dependent on the expected functional anatomy, with SOG (representing occipital cortex) showing a relatively larger target peak (although 'planning' and 'execution' peaks in the right cortex), pIPS showing roughly equal target, planning, and execution peaks, and mIPS and PMd showing predominant execution peaks. Third, the degree of reach task-specificity (gap between black vs. grey lines) generally increased both in time from the target response to the execution response and in cortical space from occipital cortex to parietal cortex to frontal cortex. Thus, the entire occipital-parietal-frontal axis was activated during target coding, planning, and execution, but the task-specificity of these responses increased along the antero-frontal axis and in the temporal transition from target, planning, and execution responses. We will examine this in more detail in the following sections using spatial parameters related to visual input, motor output, and visuomotor transformation.

Motor and Visual Selectivity during Movement Planning

We next focused on the question of whether spatially selective activation during reach planning encodes retrospective target information and/or prospective movement information (Curtis, 2006). After the pro or anti-instruction, participants might hypothetically still retain memory of target location (left or right), while simultaneously planning a movement in the same or opposite direction. We took advantage of this to create contrasts that utilized all of the planning data, and either highlighted 1) visual direction selectivity where the pro-anti movement selectivity should cancel out (as in the right-target example shown in the left column of Figure 4A) or 2) movement direction selectivity, where left-right target direction should cancel out (as in the rightward movement example shown in the right column of Figure 4A). Consistent with some previous studies (Connolly et al., 2003; Fernandez-Ruiz, 2007; Bernier et al., 2012; Gertz and Fiehler, 2015) we only found contralateral directional tuning in reach-related areas located within the left hemisphere (opposite to the reaching hand). These areas are shown in Figure 4B, C (with corresponding ß-weights provided in Supplementary Figure 2 and Talairach coordinates in table 4). Some other regions of ipsilateral sensitivity appeared in both hemispheres in regions not generally associated with reach; these were eliminated from further analysis.

Visual Target Direction Selectivity: Contrast 4 [(pro-reach right target + anti-reach right target) – (pro-reach left target + anti-reach left target)] investigated visual selectivity, as trials where the visual target was presented in the right visual field were contrasted from trials where the visual target was presented to the left, regardless of the motor goal. In this contrast, the left cuneus was the only area to show significant contralateral activation for visual target direction (Figure 4B). A similar contrast was

performed on the right hemisphere [(pro-reach left target + anti-reach left target) – (pro-reach right target + anti-reach right target)] but failed to yield significant activation that met our localizer criteria

Movement Direction Selectivity: Contrast 5 [(pro-reach right target + anti-reach left target) – (pro-reach left target + anti-reach right target)] investigated motor selectivity, as trials where the motor goal was to the right were contrasted from trials where the motor goal was to the left, regardless of the initial visual presentation. This contrast revealed widespread contralateral movement selectivity in occipital, parietal, and frontal areas (Figure 4C), including primary visual cortex (V1), lingual gyrus (LG), superior occipital gyrus (SOG), superior parietal occipital cortex (SPOC), midposterior intraparietal sulcus (mIPS), anterior intraparietal sulcus (aIPS), precuneus (PCu), angular gyrus (AG), dorsal premotor cortex (PMd), medial primary motor cortex (mM1), and an area bordering on primary motor and somatosensory cortex (M1/S1). This illustrates a network of reach-associated areas concerned with specifying upcoming reach direction during the planning phase. A similar contrast was performed on the right hemisphere [(pro-reach left target + anti-reach right target) – (pro-reach right target + anti-reach left target)] but failed to yield significant activation that met our localizer criteria.

Temporal Evolution of Visual Direction vs. Motor Direction Coding.

One of the main aims of our visually and movement direction selective voxelwise contrasts was to localize reliable visuomotor regions for a more detailed temporal analysis on their time course data. This allows us to understand the time course of visual and motor selectivity both within and across cortical sites. In these analyses, we traced the entire time course of visual and movement selectivity in the areas shown in Figure 4 using both the visual direction contrast (contrast 4) and the movement direction contrast (contrast 5). We also did the same for 4 sites in the left hemisphere obtained independently from the analysis in Figure 2, and obtained nearly identical results (Supplementary Figure 3).

Visual direction vs. Movement direction Time Courses: Figure 5 plots the time courses of the visual direction contrast (black lines) and movement direction contrast (gray lines) for every region identified in Figure 4, with the exception of aIPS which showed relatively flat responses and is associated more with grasp than reach transport (Culham et al., 2006). One-sample t-tests ($p<0.05$) were performed to compare the % BOLD signal change at the time of the peak visual and motor activation to zero to indicate significant directional tuning in either the visual or motor domain (○). We limited our comparisons to these two points in time to show the presence of visual or motor direction selectivity in a brain area without needing to correct for multiple comparisons across timepoints. Our occipital, parietal, and frontal areas are divided into three columns for easier comparison, with 'early' to 'late' areas organized top to bottom. Again, several trends emerge from this time-course analysis. First, whereas reach general activation followed three peaks of event-related responses (Figure 3), directional selectivity showed only two peaks: the first a visual peak aligned with target

presentation, and the second a more prolonged movement peak that in most cases appears to arise late in the planning phase, dropping off just at execution. Second, although visual peaks are more predominant in the occipital areas as one would expect, the motor peak was widespread. In particular, occipital areas SOG and LG show a surprisingly robust 'movement direction tuning' during the planning phase (we will propose an alternative explanation for this in the discussion). In summary, it appears that movement direction selectivity engages the entire occipital-parietal-frontal reach network.

Even though no areas in the right hemisphere met our localizer criteria, we performed a similar analysis on right SOG, mIPS, SPOC, and PMd by flipping the Talariach x coordinate and creating a 5mm sphere ROI. These values were similar to right hemisphere coordinates for these areas from this paper and others. This is included as Supplementary Figure 4.

Visuomotor Transformations through Time: If one subtracts contrast #4 (visual direction tuning) from contrast #5 (motor direction tuning) this essentially reduces to contrast #6 [anti-reach left target – anti-reach right target]. This provides a single parameter that, applied to each time series for areas in the left hemisphere, traces the development of visual direction coding to movement direction coding in the anti-reach task, where negative represents target direction coding and positive represents movement direction coding. Figure 6 shows this analysis for 8 areas in the left hemisphere that have been selected to best represent the occipital-parietal-frontal reach network, ordered to correspond roughly to 'early' (V1) through 'late' (M1) visuomotor areas. Again, we performed paired t-tests between the motor and visually selective data

at the time of peak visual (the minimum mean value) and peak motor (the maximum mean value) selectivity to indicate significantly higher visual or motor selectivity, respectively.

As one might predict, only visual selectivity reached significance for V1, and motor selectivity for mM1, but some areas between showed some combination of both (SOG, PMd). Also, as one should expect in the anti-reach task, the switch from visual coding to movement coding occurs around the time of the pro-anti instruction (although we could not establish this statistically because of the size of variance relative to the small visuomotor scores at this cross-over point). What is more remarkable, is the strong resemblance between these curves obtained from very different brain areas, ranging from some that have been categorized as strictly visual (V1) through various visuomotor areas to M1. The next section further quantifies these observations.

Temporal correlation of direction selectivity between cortical areas

To quantify some of the qualitative observations made above, we performed temporal correlations of visual, motor, and visuomotor directional selectivity between the regions identified in Figure 4. To do this, we used the % BOLD signal change time series data from 12 seconds before the onset of movement planning (target presentation) to 12 seconds after (peak activity for motor execution as seen in figure 3). Note, that the main contribution to these correlations likely came from the target coding phase and late planning phase for the visual and motor parameters respectively (Figure 5), whereas the visuomotor parameter was modulated throughout the entire sequence (Figure 6).

Figure 7a shows the visual target direction selectivity correlations for each brain area compared to V1. V1 was selected as the most obvious reference region for visual input to the system, and the functional region from contrast 5 was used. Correlations are sorted from highest to lowest, starting from V1/V1 (black) as a reference. This shows a progressive drop in correlation (as one might expect) progressing generally from the most visual areas toward mM1. These correlations were significant for LG, SOG, AG, mIPS, M1/S1, aIPS, PMd, AG, and SPOC, but not mM1 or PCu ($p < 0.05$ with Bonferroni corrections for 10 comparisons).

Figure 7b similarly shows the movement execution direction selectivity correlations for each brain area compared to mM1. In this case, mM1 was chosen as the most obvious reference region for motor output from the system, and the functional region from contrast 5 was used. Here, correlations were ordered from lowest to highest (mM1, black bar). This resulted in a similar ordering as Figure 7a, except for a few regions (notably PCu) shifted to the left (meaning its correlations rank remained low) or right (e.g., SOG, meaning that it retained its relatively high rank in both representations). In this case, only AG, PMd, SOG, SPOC, LG, and M1/S1, but not mIPS, were significantly correlated to mM1 ($p < 0.05$ with Bonferroni corrections for 10 comparisons).

Figure 7c provides a similar plot, but in this case using the visuomotor directional parameter from figure 6. In this case there is no obvious reference region or order. Here, we used SPOC as a reference because it showed a significant correlation in both the visual and motor correlations (Figure 7a, b) and recent fMRI and TMS studies have implicated SPOC as a visual reaching area (Filimon et al., 2009; Vesia et al., 2010).

Arbitrarily, the data is ordered in figure 7c as in Figure 7b. In contrast to both of the preceding plots, in this case every region was significantly correlated to SPOC (black bar) ($p < 0.05$ with Bonferroni corrections for 10 comparisons).

When these values were calculated between all possible pairings of our identified regions of interest, we obtained overall r values of 0.739±0.13 for visual, 0.652±0.20 for motor, and 0.799±0.10 for visuomotor (mean ± SD) selectivity indices. To test if they were significantly higher than zero, we preformed three one-sample t-tests on the mean r scores for each brain area, comparing zero to visual ($t(10)=37.129$, $p>0.001$), motor ($t(10)=18.771$, $p>0.001$), and visuomotor ($t(10)=45.755$, $p>0.001$) selectivity frames, all of which were highly significant. To test for differences between selectivity frames and to investigate differences between brain regions, we performed an ANOVA on the r values with selectivity frame (visual, motor, and visuomotor) and the 11 brain areas as fixed factors. The ANOVA was significant ($F(32,1)=5.689$, $p<0.001$) and showed significant main effects for selectivity frame ($p<0.001$) and brain area ($p<0.001$), as well as a significant interaction between selectivity frame and brain area ($p<0.005$). Bonferroni post-hoc tests on selectivity frames revealed that visual, motor, and visuomotor selectivity were all significantly different from each other. Thus, both retrospective target direction and prospective reach direction were important for describing correlations between these networks at different phases, and a visuomotor parameter that captured both of these provided the best overall description. Bonferroni post-hoc tests on brain areas revealed that the precuneus and V1 showed significantly lower correlations than several other brain areas (for PCu: AG, aIPS, mM1, mIPS, PMd, M1/S1, SOG, and SPOC; for V1: AG, mIPS, PMd, M1/S1, SOG, and SPOC).

Figure 8 graphically summarizes the results of our visual direction (a), motor direction (b), and visuomotor directional (c) correlations (derived as in Figure 7) between all of the regions of interest from Figure 4, and uses these as a measure of the spatial coordination of these modules (and perhaps direct / indirect connectivity). The purpose of this figure is to illustrate that sensory motor transformations are carried out by a large network, and not just a couple of regions of interest as reported in many studies. The width of each line is scaled by the r^2 value for the two regions that it joins, with significant correlations highlighted in yellow ($p < 0.05$, non-significant correlations are shown in orange). This identifies 'hub' areas with thick yellow lines (high correlations and significance) in each domain (sensory, motor, or sensorimotor) from an area with thin orange lines (low correlations and significance). For target direction selectivity (arising mainly during the visual coding phase; Figure 8 a), one observes an extensive network of significant correlations including V1, SOG, mIPS, M1/S1, and PMd (i.e. these areas have many thick yellow lines), but largely excluding mM1 and PCu (i.e., these areas have mainly thin orange lines). For movement direction selectivity (arising mainly during the late planning phase; Figure 8 b) a network of significant correlations arose between the regions spanning SOG to M1, including AG, SPOC, M1/S1, and PMd, but excluding the very thin 'connections' to the early visual areas V1 and LG, as well as parietal areas aIPS, mIPS and PCu. In contrast, for the visuomotor parameter, (Figure 8 c), nearly all of the correlations are robust and significant (with PCu remaining the main exception). These analyses again suggest that, despite overall biases toward visual or motor function between different sites, the entire occipital-parietal-frontal reach network is involved in the visuomotor transformation for a memory-guided reach task.

Discussion

In this study, we used an event-related fMRI design to investigate several key questions. To summarize, the first was to differentiate which cortical areas are involved in spatial target representation, reach movement planning, and reach movement execution. This analysis revealed selective, bilateral PMd and right pIPS activation during the target representation phase, whereas an entire occipital-parietal-frontal reaching network was activated during the motor planning and execution phases. The second question we aimed to answer was, during motor planning, which brain areas are directionally selective in visual or motor coordinates? During our planning phase, the left cuneus showed significant contralateral visual selectivity, but the majority of directionally selective occipital, parietal and frontal activation was tuned for contralateral reach direction. Observing the time courses of these directional parameters across all three phases of our task, we observed that most areas showed visual selectivity following target presentation and most areas showed movement selectivity late in the planning

phase, but all reach-related areas showed a progressive visuomotor transition when these measures were collapsed into a single visuomotor parameter. Likewise, when we correlated these parameters through time between different areas, we found overlapping but distinct visual and motor networks, but that all of the areas activated in occipital, parietal, and frontal cortex were correlated in terms of the visuomotor index. In the following sections we will discuss each of these findings in more detail.

General activation during target memory, planning, and execution.

Many previous fMRI studies have implicated superior occipital-parietal-frontal cortex in visually guided reaching (Astafiev et al., 2003, Connolly et al., 2003; Medendorp et al., 2003, 2005; Prado et al., 2005; Fernandez-Ruiz et al., 2007; Beurze et al., 2009; Cavina-Pratesi et al., 2010; Fabbri et al., 2012; Konen et al., 2013; Chen et al., 2014). However, to our knowledge none of these clearly separated the three phases of target representation, motor planning, and motor execution through time. To do this within the spatiotemporal limitations of fMRI, we required a paradigm with a series of instructions and delays which likely introduced more cognitive aspects to the task one would see during on-line control, but with this caveat in mind, we were able to trace both general and direction-specific activation through those three phases. Most of our regions of interest showed different degrees of time-locked activation during target representation, planning, and execution (Figure 3), depending on whether the region was more visual (e.g., SOG) or motor (e.g., PMd) but here we will restrict our discussion to significant clusters of activation during these three phases (Figure 2).

Our analysis of the target representation phase (Figure 2 a) revealed limited activation in bilateral PMd and right pIPS, perhaps related to spatial working memory (Courtney et al., 1996; Srimal and Curtis, 2008) or activity related to preparatory set (Culham et al., 2006, Chen et al., 2014). Chen et al. (2014) found a broader range of occipital-parietal-frontal activation during the target memory phase of their paradigm. However, our target memory phase was followed by target planning before execution, whereas their target memory phase was followed immediately by motor execution, so this may have precipitated earlier preparatory activity in their paradigm. Activation in the parietal cortex is consistent with the uncertainty condition found in Gertz and Fiehler (2015), though their parietal activation was in the left hemisphere and ours was in the right. This difference could be due to the additional delay we added before the pro / anti instruction or the way we defined regions of interest (we derived coordinates from peak voxels in our own data whereas they used published coordinates).

Note that in our paradigm, subjects could not anticipate the required movement plan or derive it from the visual stimulus until the pro / anti instruction was given at the start of the second delay. During this motor planning phase (Figure 2b), we observed widespread activation in the classic parieto-frontal reach network, including SPOC, mIPS, SMA, PMd, and M1 (Culham et al, 2006; Gallivan and Culham, 2015). Comparing this widespread planning activation to the limited activation that was observed in the target representation phase suggests that previous studies that combined these two phases (Medendorp et al., 2003, Fernandez-Ruiz et al., 2007) were mainly reporting activity related to visuomotor transformations and / or movement planning, as opposed to target memory. We also observed considerable activation of

occipital cortex, including LG, IOG and SOG, during the second delay, a phenomenon known as ‘occipital reactivation’ (Singhal et al., 2013), which we will discuss further in subsequent sections. In all these lobes, lateral cortex activation was greater in the left hemisphere contralateral to the hand, consistent with previous studies (Connolly et al., 2003; Fernandez-Ruiz, 2007; Bernier et al., 2012; Gertz and Fiehler, 2015). Finally, all of these regions of activation became even more extensive (relative to controls) in the motor execution phase (Figure 2 c), also extending into prefrontal (e.g. IFG) and inferior parietal (e.g. SMG) areas that might be associated with cognitive aspects of the task, such as guidance of the movement based on spatial memory (Gallivan et al., 2015). In general, through our three phases we observed a general spread and ramping up of activation relative to controls throughout occipital-parietal-frontal cortex, presumably as different constraints were added to the task (target memory, rule based visuomotor transformation, motor planning, and actual execution) while retaining past information.

Directional Selectivity during Movement Planning

A second goal of our study was to look at cortical direction selectivity during movement planning, and determine which areas are selective for visual target direction versus movement direction. Here we will restrict our discussion to regions that showed significant clusters of activation. One of the main aims of our visually and movement direction selective contrasts was to localize reliable visuomotor regions for a more detailed temporal analysis on their time course data. We further restricted this analysis to the second delay (movement planning) because 1) this gave much more activation in general than the first delay, 2) the first delay could only yield visual directional

selectivity, whereas 3), selective combinations of our pro and anti-reach data could isolate visual vs. motor selectivity during the second delay. We will discuss these together, then separately.

Contralateral Direction Tuning and Handedness. Although we found scattered, non-specific clusters of activation of ipsilateral tuning (for either target or movement, primarily in the right hemisphere) in general, we found fairly widespread contralateral direction tuning within the occipital-parietal-frontal reach system. This generally agrees with previous investigations based on fMRI (Medendorp et al. 2003; 2005; Filimon, 2010; Vesia and Crawford, 2012; Gertz and Fiehler, 2015), MEG (Van Der Werf et al., 2010), TMS (Vesia et al. 2010), patients (Khan et al., 2007) and primate neurophysiology (Gail and Andersen, 2006; Gail et al., 2009; Westendorff et al., 2010). Further, this contralateral tuning was always in the left hemisphere, contralateral to the right hand used in the study. This is consistent with several previous fMRI studies (Connolly et al., 2003; Fernandez-Ruiz, 2007; Bernier et al., 2012; Gertz and Fiehler, 2015). This asymmetry of responses is thought to be due to interactions between hand lateralization and visual hemifield lateralization (Perenin and Vighetto, 1988; Rossetti et al., 2003, Medendorp et al., 2005b; Beurze et al., 2007; Blangero et al., 2007, Vesia and Crawford, 2012). Also, previous studies have shown that reach-related areas show enhanced activation in the left hemisphere for targets in the region of space one usually acts (Gallivan et al., 2011). Also, fMRI studies that have looked at spatial tuning in parietal cortex and reaching with both hands found that these effects interact (Medendorp et al., 2005). Thus the left hemisphere shows the strongest directional tuning for right hand and right hemisphere for left hand (which we did not test). Thus it is

likely that we, like others before us who used right hand movements, cannot expect a strong directional effect in the right hemisphere.As right handed participants usually act on objects in the right visual space and we only scanned right handed participants, this may help explain this result. In more visual areas, this may also be due to attentional enhancement of visual stimuli near the hand (Reed et al., 2006; Abrams et al., 2008). The reach starting position used in our task just left of the subjects midline may also have lead to a slight increase in activation for rightward reaches, as those movements were of a slightly larger amplitude. This was done to minimize head movement artifacts in the scanner by restricting upper arm movement, but it is possible that this influenced results.

This activation may also be due to the statistics of fMRI, as an area requires both a hand preference and a visual field preference to sum to reach a significant BOLD effect. It does not imply that there is no activity at the physiological level, but simply that the activation doesn't meet our exclusion criteria. To investigate this a bit further, Supplementary Figure 7 shows the visually and motor direction time course activation for right SOG, IPS, SPOC, and PMd. While most of the % signal change is near zero, right SOG shows some early visual selectivity consistent with what we found in left SOG.

Visual directional selectivity. Our visual directionally selective contrast in our task found that only the left cuneus showed significant activation for visually contralateral targets regardless of the motor requirement. This implies that there is a region in occipital cortex that is specifically concerned in retaining the visual direction of the original stimulus, regardless of whether subjects are planning a movement in that

direction or in the opposite direction. Makino et al. (2004) previously found that the cuneus can be activated by both visual search and memory search, and suggest that it may be responsible for attentional shifts in short and long term memory. These search and attentional functions may be aided by a visual representation of an object in space, regardless of and independent from the motor requirement of a task. Nonetheless, the extent of visual lateralized activation that we observed here, restricted to cuneus, was rather modest compared to the visually-tuned BOLD response observed throughout occipital and parietal cortex during reversing prism adaptation (Fernandez-Ruiz et al. 2007). We will return to this apparent contradiction in a later sub-section.

Movement direction selectivity. During movement planning, we observed relatively widespread movement-tuned direction selectivity in parieto-frontal cortex, including mIPS, SPOC, AG, aIPS, PMd, and M1/S1. This generally agrees with previous reach (and or saccade) investigations that have used the pro-anti task combined with fMRI (Medendorp et al. 2005), MEG (Van Der Werf et al., 2008, 2010), and primate neurophysiology (Gail and Andersen, 2006; Gail et al., 2009; Westendorff et al., 2010). Consistent with this, PMd neurons are active during the delay period preceding an instructed movement, as well as tuned for the direction and distance of reaches with either hand (Weinrich and Wise, 1982; Caminiti et al., 1991; Messier and Kalaska, 2000; Cisek et al., 2003). It is perhaps more surprising that we found several occipital areas linked to movement direction during the planning phase, including SOG. Likewise, Chen et al. (2014) found directionally selective occipital activation during their movement execution phase. One does not generally associate occipital cortex with movement planning, but note that in the pro / anti paradigm, subjects may use a

strategy of imagining a target that is either contiguous with, or opposite to the original visual stimulus. These findings suggest that occipital cortex plays a more important role in action planning than is often assumed (Pasternak and Greenlee, 2005; Gutteling et al., 2015).

Reconciling Studies of Spatial Tuning for Reach Planning. Returning to the Fernandez-Ruiz et al. (2007) prism reversal study, which showed visual tuning in most of the same occipital-parietal regions that showed movement tuning in the pro / anti reach task (see also Gertz and Fiehlher 2015). This appears to be a contradiction, but Ferandez-Ruiz et al. (2007) offered an explanation based on discriminating the parameter being represented (i.e., visual target, vs. movement goal, vs. movement direction) and the coordinate frame used to represent this (i.e., retinal coordinates vs. body-fixed coordinates). According to this notion, areas such as mIPS do not encode visual target direction (that contradicts the current study) or movement direction (which contradicts the prism-reversal study). Instead, they may encode the direction of the imagined goal in retinal coordinates (which would be linked to retinal input during prism reversal, but reversed relative to retinal input in the anti-reach task). This model fits most of our occipital-parietal regions, with exception of cuneus (which appears to encode visual stimulus direction in both tasks; see above) and AG, which appears to encode extrinsic movement direction in both tasks, perhaps in somatosensory coordinates (Fernandez-Ruiz et al. 2007; Vesia et al. 2006, 2010; Vesia and Crawford 2012).

A complication to this scheme is that Kuang et al. (2016) recorded action potentials from intraparietal cortex in monkeys trained on both the prism reversal task

and pro / anti reach task, and found that some neurons did encode the goal in visual coordinates, but most encoded movement direction. They reconciled this finding with fMRI results by noting that local field potentials –which may drive the BOLD response – agreed better with the visual goal prediction. Alternatively, the massive amount of training required for monkeys to do such tasks may have altered synaptic organization, whereas the human subjects received minimal training. However, these are matters of degree, not fundamental differences. Either way, it appears that the occipital-parietal-frontal reach planning system can simultaneously encode three spatial variables: visual stimulus direction, the goal in visual coordinates, and extrinsic movement direction.

Visual, Motor, and Visuomotor Selectivity Through the Entire Task

Some of the most interesting findings in this experiment derived from plotting the time courses of visual and motor selectivity (Figure 5) for all of our regions of interest. A number of neurophysiological studies have followed the time course of directional tuning during a pro / anti task (e.g. Zhang and Barash, 2000; Gail and Andersen, 2006; Gail et al., 2009). However, to our knowledge, we are the first to extract these variables from pro / anti reach data in the human brain and examine their time course through separate target representation, planning, and reach execution phases. Although fMRI suffers by comparison in spatiotemporal resolution, it compensates by allowing one to compare these responses across the entire brain. In short, although some areas showed primarily visual direction tuning following presentation of the target and some primarily showed movement direction tuning late in the planning phase, most of our regions of

interest showed both of these responses. We shall consider these 'lobe-by-lobe', and then consider the network.

Occipital cortex. Not surprisingly V1 and cuneus primarily showed visually selective activation, as numerous previous studies have shown human V1 to code visual stimulus responses (Engel et al., 1997; Singh et al., 2000), and perhaps even visual memory responses (Pratte and Tong, 2014; Malik et al., 2015). Visual selectivity in cuneus during motor planning is also consistent with previous findings that that parieto-occipital areas like SPOC show enhanced activation in the left hemisphere for targets in the region of space one usually acts (Gallivan et al., 2011). As right handed participants usually act on objects in the right visual space and we only scanned right handed participants, this may help explain this result. However, SOG and LG showed both visual and 'motor' selectivity. It is possible that these structures initially responded to the visual stimulus, but after the pro-anti instruction were involved in imagining a virtual target that could be flipped opposite to the actual stimulus in the case of anti-reach trials. This could explain the phenomenon of occipital reactivation during reaches, and could involve re-entrant feedback from motor systems (Singhal et al., 2013).

Parietal cortex. To different degrees, all of our parietal structures showed dual spatial selectivity, but SPOC and AG stood out as areas that showed both visual and motor selective activation. Consistent with our results, recent studies have implicated SPOC as a visually-guided reaching area (Culham et al, 2006; Filimon et al., 2009; Vesia et al., 2010; Gallivan and Culham, 2015). Previous studies on AG, however, have implicated it as coding the motor output of a task (Fernandez-Ruiz et al., 2007; Vesia et al., 2010), making the visually selective activation unexpected. However, this

might indicate transformation of visual signals into somatosensory signals, as suggested by its general role in left-right space discrimination (Hirnstein et al., 2011).The Precuneus was found to only be mainly visually selective during the target representation phase. This activation could be related to visuo-spatial imagery (Cavanna and Trimble, 2006), although it did not show the anti-reach reversal we observed for LOG. It is also unclear why both PCu and SPOC show slight reversals from motor to visual planning around the time motor planning begins. We speculate this may be due to a visual re-activation once the movement is known. It was somewhat surprising that mIPS only showed directionally selective motor activation given that it has been linked to both reach and saccade planning, attention, and visual working memory (Curtis et al., 2004; Srimal and Curtis, 2008; Curtis and Connolly, 2008; Jerde et al., 2012). Medendorp (2005) found that for saccades, retinotopic IPS (similar to mIPS) coded the visual location of a target before the pro/anti instruction and the motor direction afterwards. It is important to note however that these areas were selected by different methods (an independent localizer versus peak voxel region of interest) and that activation for saccades may differ from the reach planning network. This result can be explained by Fernandez-Ruiz et al., 2007, where after prism adaptation the visual goal corresponded to the reversed image that was seen, and this was then transformed into the opposite direction downstream. In our task, for anti-pointing the visual goal is imagined as being opposite to what is seen and then corresponds to movement direction, which may explain the presence of only motor selectivity.

Frontal cortex. Left PMd showed visually selective activation during target representation and motor selectivity during movement execution. Previous research

has found left PMd activation for right arm reaching (Medendorp et al., 2005; Bernier et al., 2012; Gertz and Fiehler, 2015) and implicated the region in transforming visuospatial information into motor codes (Medendorp et al., 2005; Beurze et al., 2007), which supports our motor-selective finding. This is also supported by non-human primate neurophysiology, where PMd has been found to encode multiple movement goals if more than one potential target exists (Cisek and Kalaska, 2002). Once a movement is selected, neurons encoding that movement plan are enhanced while neurons encoding alternatives are suppressed (Cisek and Kalaska, 2005). There is also evidence from multivariate fMRI techniques for target selective coding in PMd (Gallivan et al., 2011; Fabbri et al., 2014), which may help explain the visually-selective encoding we noted during the target representation phase.

Visuomotor Selectivity in *all* Areas. One of our more striking findings was that when we described our occipital-parietal-frontal regions with the use of a visuomotor parameter (derived from the anti-reach data) and plotted these data through the entire time course of our task (Figure 6), every single area, from V1 to M1, looked remarkably similar (with the exception of a mid-task 'bump' in some areas like precuneus, around the time of the pro-anti instruction). This appears to illustrate a very simple but profound message: despite the many functional differences between these areas (like those described above and by many other authors), an entire occipital-parietal-frontal network is engaged in the transformation of visual stimuli into motor acts; Not only at different serial stages of processing, but through the entire duration of the task (for example see the occipital reactivation in our SOG data). In this sense, even though visuomotor transformations can be observed within single structures and even single neurons (e.g.,

Sajad et al. 2015, Sadeh et al. 2015), almost the entire cortex is engaged in the entirety of such transformations.

Spatiotemporal Correlations for Visual, Motor, and Visuomotor Selectivity

We were able to quantitatively summarize our measures of early visual tuning and late motor tuning, and organize these into spatiotemporally correlated modules by correlating these measures through time between left hemisphere regions of interest (Figure 7a, b) and using these correlations to construct a network of spatiotemporally correlated modules (Figure 8a, b). This resulted in two widely distributed, overlapping networks, the first strongly correlated to visual input from V1 (Figures 7a, 8a), and the second strongly correlated with motor output from M1 (Figures 7b, 8b). However, it was the visuomotor parameter that yielded the best overall correlations between areas (Figures 7c, 8c). Note that these data (Figure 7A-C) only show visuomotor correlations for one example area. The full set of sensory, motor, and sensorimotor correlations for all areas are illustrated graphically in Figure 8. Although correlation does not imply causation (for example, some of these correlations may have been due to common inputs or some attentional processing in the brain), the structure of these networks appear to agree well with the known anatomy of the dorsal visual stream system and reach systems (Vesia et al., 2012; Gallivan et al., 2015). Further, it suggests that the entire network is concerned with transforming retrospective visual direction into prospective movement direction (Curtis 2006).

Of these areas, SPOC was the only shared region that significantly correlated with all other areas in the visuomotor parameter shown in figure 8c, which is based on the full dataset showing the correlations between all areas. This suggests that SPOC is a major hub in this network and seems consistent with SPOC having a prominent role in representation of target location for reach (Vesia et al., 2010; Vesia and Crawford 2012). However, several other areas (LG, SOG, M1/S1, PMd, and AG) significantly correlated to both V1 in the visual domain and mM1 in the motor domain, so this transformational role is not unique to one area. Nor is this unique to dorsal parietal cortex, as AG –an inferior parietal area— also showed significant visual correlation with V1, motor correlation with mM1, and visuomotor correlations with most areas (AG was also highly correlated with most of the other brain regions, however it was not significantly correlated with V1 or PCu) although its overall visual connectivity was less than its motor connectivity. Together with its multiple roles in coding motion in external space (Fernandez-Ruiz et al. 2007; Vesia and Crawford 2012), discrimination of left space from right (Hirnstein et all 2011), controlling multiple effectors (Vesia et al. 2010), and in agency (Farrer et al. 2008), this might suggest that AG plays a central role in monitoring the awareness of ones actions within external space. In comparison, our current data suggest that other sensory areas like cuneus and SOG may be more concerned with monitoring events and goals in visual space. This again is consistent with the notion that the brain simultaneously monitors space in multiple frames. Finally, out of all of our ROIs, PCu showed the weakest connectivity in all spatial domains, but this may be task specific, e.g., PCu has been implicated in allocentric functions (Uchimura et al. 2015; Chen et al. submitted), whereas our task was strictly egocentric.

Overall, these data suggest that the brain uses a broadly distributed, common visuomotor code for memory guided reach, and thus the need for so many network nodes likely arises from other cognitive demands.

The role of Attention

It is very important to acknowledge that our paradigm does not disambiguate attention from motor signals. It only disambiguates visual direction tuning from motor direction. It is likely that subjects attend to remembered target direction in the first memory delay (consistent with Rizzolatti et al., 1987), and goal direction in the second planning delay, switching this to the opposite hemifield during the 'anti' trials, as suggested by Rolfs et al. (2013). Thus attention could contribute the strong correlations between visual (stimulus direction) tuning, motor (movement) direction tuning, and visuomotor (goal) direction tuning. However, there are other aspects of our results that spatial attention cannot explain by itself. First, spatial attention alone cannot explain the hemispheric asymmetries that we and others observe (this is addressed in the next section). Second, spatial attention alone would only predict a switch from stimulus vs. movement tuning between the memory and planning delay, whereas we see massive recruitment of additional areas associated with motor control (Fig 2), with directional tuning in many of these (Figure 4). In most motor control, investigators would balk at the notion that attention is unlikely to be the primary driver of directional responses in areas such as premotor cortex and M1. To some extent this is also true for our parietal areas., Indeed for example we have previously also shown that TMS over SPOC, mIPS, and AG during a memory/planning delay influences reach behavior (Vesia et al. 2010). The current paradigm is designed to show spatial direction tuning and cannot separate

attention from memory or planning (if that is possible), but we would not go as far as to say that memory and planning are ‘just attention’.

Table 1. Talairach coordinates and number of voxels for Target Representation regions of interest

Area	Mean X	Mean Y	Mean Z	Voxels
Left PMd	-25.43	-10.48	52.47	976
Right PMd	20.61	-9.4	51.53	976
Right pIPS	21.64	-61.84	48.21	909

Table 2. Talairach coordinates and number of voxels for Movement Planning regions of interest

Area	Mean X	Mean Y	Mean Z	Voxels
Left SOG	-13.47	-89.31	14.38	959
Right SOG	24.31	-79.24	26.31	935
Left IOG	-44.32	-79.63	-0.47	696
Left LG	-10.5	-77.5	-12.5	1000
Right LG	7.5	-74.5	-12.5	1000
Left mIPS	-24.5	-44.5	52.5	1000
Right mIPS	22.5	-46.5	44.5	1000
Left pIPS	-18.5	-68.5	38.5	1000
Right pIPS	18.5	-59.5	45.5	1000
Left SPOC	-22.41	-73.51	32.58	979
Left PMd	-15.5	-14.5	58.5	1000
Right PMd	23.5	-14.5	56.5	1000
Left PMv	-51.47	-5.51	34.47	964
Right PMv	45.51	-2.53	31.44	964

Left CMA	-7.5	-23.5	49.5	1000
Right CMA	8.5	-26.5	48.5	1000
Left SMA	-7.5	-9.5	54.5	1000
Right SMA	10.5	-4.5	45.5	1000
Right S1	16.5	-34.5	58.5	1000
Left M1	-15.51	-26.49	61.49	997

Table 3. Talairach coordinates and number of voxels for Movement Execution regions of interest

Area	Mean X	Mean Y	Mean Z	Voxels
Left IOG	-51.42	-65.21	-4.27	722
Right IOG	46.5	-60.5	-7.5	1000
Left pIPS	-8.11	-65.31	51.09	582
Right pIPS	13.78	-70.79	46.53	579
Left mIPS	-24.5	-44.5	52.5	1000
Right mIPS	22.5	-46.5	44.5	1000
Left SMG	-52.5	-23.5	19.5	1000
Right SMG	52.5	-20.5	32.5	999
Left PMd	-25.6	-6.1	55.3	1000
Right PMd	23.5	-5.5	58.5	1000
Left PMv	30.46	42.46	31.46	990
Right PMv	-34.5	41.5	25.5	1000
Left IFG	-57.85	1.84	18.67	835
Right IFG	55.44	9.53	4.56	986
SMA	-4.5	-12.5	51.5	1000
Left S1	-25.5	-23.5	61.5	1000
Left M1	-20.5	-17.5	65.5	999

Table 4. Talairach coordinates and number of voxels for contralateral visually and motor selective areas during movement planning in the left hemisphere

Area	Mean X	Mean Y	Mean Z	Voxels
Visually Selective				
Cuneus	-2.56	-77.12	14.67	691
Motor Selective				
V1	-7.46	-76.05	-0.52	798
SOG	-28.51	-83.51	15.51	998

LG	-21.44	-74.43	-14.49	985
mIPS	-25.36	-45.39	58.35	961
SPOC	-24.6	-73.82	35.33	716
aIPS	-33.58	-27.39	50.78	902
Pcu	-4.46	-62.81	49.69	767
AG	-60.91	-36.32	24.07	823
PMd	-25.61	-3.38	58.67	671
mM1	-4.22	-17.19	63.32	859
M1/S1	-30.38	-16.12	56.13	891

Figure 1. Experimental setup and paradigm. **A*)*** Photograph of The experimental setup.

B) Illustration of the experimental paradigm. The display of visual targets is the same for all three tasks (Pro-Reach, Anti-Reach, and Colour Report). The key difference between the two reach tasks is the congruence of the visual target and motor goal. In the Pro-Reach task, subjects reach towards the remembered location of the previously displayed visual target. In the Anti-Reach task, subjects reach towards the location mirror symmetrical to the visual target in the opposite visual field. As the target presentation and pro/anti instruction are separated by an 8 second delay, this allows the task to disentangle target representation from motor planning and execution. In the Colour Report task, target colour (red or green) rather than location is remembered and reported.

Figure 2. A) Voxelwise statistical maps obtained from the RFX GLM for the contrast Pro-Reach + Anti-Reach > Colour report. Event-related group activation maps are

displayed on the inflated brain of one representative subject for target representation. The leftward inflated brain represents the left hemisphere, and the rightward brain represents the right hemisphere. Highlighted areas show significantly higher activation than control data with a $p>0.05$ with Bonferroni and cluster threshold corrections. These areas include the left and right dorsal premotor cortex (PMd) and right posterior intraparietal sulcus (pIPS). B) Voxelwise statistical maps obtained from the RFX GLM for the contrast Pro-Reach + Anti-Reach > Colour report. Event-related group activation maps are displayed on the inflated brain of one representative subject for motor planning. The two leftward inflated brains represent the left hemisphere, and the two rightward brains represent the right hemisphere. Highlighted areas show significantly higher activation than control data with a $p>0.05$ with Bonferroni and cluster threshold corrections. These areas include bilateral dorsal premotor cortex (PMd), ventral premotor cortex (PMv), midposterior intraparietal sulcus (mIPS), posterior intraparietal sulcus (pIPS), and superior occipital gyrus (SOG). Significant activation was also observed in left primary motor cortex (M1), superior parietal occipital cortex (SPOC), and inferior occipital gyrus (IOG), and right primary somatosensory cortex (S1). C) Voxelwise statistical maps obtained from the RFX GLM for the contrast Pro-Reach + Anti-Reach > Colour report. Event-related group activation maps are displayed on the inflated brain of one representative subject for motor execution. The two leftward inflated brains represent the left hemisphere, and the two rightward brains represent the right hemisphere. Highlighted areas show significantly higher activation than control data with a $p>0.05$ with Bonferroni and cluster threshold corrections. These areas include bilateral dorsal premotor cortex (PMd), midposterior intraparietal sulcus (mIPS),

supramarginal gyrus (SMG), inferior occipital gyrus (IOG), the supplementary motor area (SMA) and inferior frontal gyrus. Significant activation was also observed in left primary motor cortex (M1) and primary somatosensory cortex (S1), and in right ventral premotor cortex (PMv).

Figure 3. Time courses for four brain areas of interest (SOG, pIPS, mIPS, and PMd) that were bilaterally active from the Motor Preparation Reach (pro + anti) > Motor Preparation Color contrast during the motor planning phase. The dark grey line indicates activity (% signal change) from reach trials and the light grey line indicates activity from colour report trials. Error bars are SEM across subjects. The x axis displays time in seconds and is time locked to the movement planning phase. The three vertical black dashed lines indicate the onset of the target representation, motor planning, and motor execution phases (from left to right). Note that there is an activation peak corresponding to the black solid lines for all 7 time courses that contain three peaks (B-H), the only exception being left SOG.

Figure 4. A) A visualization of the visual target and motor goal selectivity contrasts used in this experiment. For the visual selectivity contrasts, trials where the target was initially presented in the right visual field were contrasted against trials where the visual target was presented to the left, independent of the direction of the movement. For motor selectivity contrasts, the opposite was the case. Trials where the motor goal was

to the right were contrasted against trials where the motor goal was to the left, independent of where the initial visual target was presented. These contrasts were used to examine activity during the movement planning phase. ***B)*** Voxelwise statistical maps obtained from the RFX GLM for the contrast Pro-Reach Right + Anti-Reach Right > Pro-Reach Left + Anti-Reach Left. Event-related group activation maps are displayed on the left hemisphere inflated brain of one representative subject for motor planning. Highlighted areas show significantly higher activation than control data with a $p>0.05$ with Bonferroni and cluster threshold corrections. The Left cuneus met these criteria. C) Voxelwise statistical maps obtained from the RFX GLM for the contrast Pro-Reach Right + Anti-Reach Left > Pro-Reach Left + Anti-Reach Right. Event-related group activation maps are displayed on the left hemisphere inflated brain of one representative subject for motor planning. Highlighted areas show significantly higher activation than control data with a $p>0.05$ with Bonferroni and cluster threshold corrections. These areas include primary visual cortex (V1), lingual gyrus (LG), superior occipital gyrus (SOG), superior parietal occipital cortex (SPOC), midposterior intraparietal sulcus (mIPS), anterior intraparietal sulcus (pIPS), precuneus (PCu), angular gyrus, dorsal premotor cortex (PMd), primary motor cortex (M1), and an area encompassing parts of primary motor and somatosensory cortices (M1/S1).

Figure 5. A plot of the time courses of visual and motor selectivity for left occipital (V1, SOG, cuneus and LG), parietal (SPOC, mIPS, Pcu, and AG), and frontal (PMd, M1/S1, and M1) left hemisphere brain regions. On the x axis, time is in scans (2 seconds each) and 0 indicates the start of the motor planning phase. The three black vertical lines

indicate the times of peak activity noted in figure 3 for the target representation (TR), motor planning (MP), and motor execution (ME) phases. The dark grey lines indicate the visually selective mean % signal change across subjects. This was calculated by subtracting the time courses for trials where the visual target was presented ipsilaterally (pro-reach left and anti-reach left) from trials where the visual target was presented contralaterally (pro-reach right and anti-reach right). The light grey lines indicate the motor goal selective mean % signal change across subjects. This was calculated by subtracting the time courses for trials with an ipsilateral motor goal (pro-reach left and anti-reach right) from trials with a contralateral motor goal (pro-reach right and anti-reach left). White open circles (○) indicate activity significantly greater than zero (one-sample t-test, $p<0.05$). Error bars are SEM across subjects

Figure 6. Coordinate-specific activity for left V1, SOG, SPOC, mIPS, AG, aIPS, PMd, and M1. This was calculated by subtracting the visual selective time course data from the motor goal selective time course data displayed in figure 5. Thus, a negative % signal change indicates visual selectivity and a positive score indicates motor goal selectivity. The three black vertical lines indicate the times of peak activity noted in figure 3 for the target representation (TR), motor planning (MP), and motor execution (ME) phases, and grey vertical lines indicate their onset. Open circles (○) indicate significantly greater coding for that coordinate system as revealed by a paired t-test ($p<0.05$). Error bars are SEM across subjects

Figure 7. Visual, motor, and visuomotor correlations. 7A) The time courses for the 10 motor-selective areas in the left hemisphere correlated for visual selectivity to V1 from target presentation (-12 seconds) to peak motor execution activation (+12 seconds), time-locked to the onset of movement planning (the visual phase). 7B) The time courses for the 10 motor-selective areas correlated for motor selectivity to M1 (from the same time period as 7a). 7C) The time courses for the 10 motor-selective areas correlated for visuomotor selectivity to SPOC. For all figures, * indicates a significant correlation ($p<0.05$) with a Bonferroni correction for 10 comparisons. Error bars are SEM across subjects.

Figure 8. The strength of correlation between left hemisphere brain areas for visual (A), motor (B), and visuomotor (C) correlations from figure 7. The thickness of the line indicates the r^2 value, with a thin line being close to 0 and a thick line close to 1. We used r^2 to increase the difference between highly correlated and less correlated areas. All r values were positive. Black areas are superficial and grey areas appear on the medial side of the inflated brain.

References:

Abrams RA, Davoli CC, Du F, Knapp WH, Paull D. 2008. Altered vision near the hands. Cognition. 107:1035–1047.

Andersen RA, Buneo CA. 2002. Intentional maps in posterior parietal cortex. Annu Rev Neurosci. 25:189–220.

Astafiev S V, Shulman GL, Stanley CM, Snyder AZ, Van Essen DC, Corbetta M. 2003. Functional organization of human intraparietal and frontal cortex for attending, looking, and pointing. J Neurosci. 23:4689–4699.

Berman R, Colby C. 2009. Attention and active vision. Vision Res. 49:1233–1248.

Bernier P-M, Cieslak M, Grafton ST. 2012. Effector selection precedes reach planning in the dorsal parietofrontal cortex. J Neurophysiol. 108:57–68.

Bernier P-M, Grafton ST. 2010. Human posterior parietal cortex flexibly determines reference frames for reaching based on sensory context. Neuron. 68:776–788.

Beurze SM, de Lange FP, Toni I, Medendorp WP. 2007. Integration of target and effector information in the human brain during reach planning. J Neurophysiol. 97:188–199.

Beurze SM, de Lange FP, Toni I, Medendorp WP. 2009. Spatial and effector processing in the human parietofrontal network for reaches and saccades. J Neurophysiol. 101:3053–3062.

Beurze SM, Toni I, Pisella L, Medendorp WP. 2010. Reference frames for reach planning in human parietofrontal cortex. J Neurophysiol. 104:1736–1745.

Blangero A, Gaveau V, Luauté J, Rode G, Salemme R, Guinard M, Boisson D, Rossetti Y, Pisella L. 2008. A hand and a field effect in on-line motor control in unilateral optic ataxia. Cortex. 44(5):560-568.

Caminiti R, Johnson PB, Galli C, Ferraina S, Burnod Y. 1991. Making arm movements within different parts of space: the premotor and motor cortical representation of a coordinate system for reaching to visual targets. J Neurosci. 11(5):1182-1197.

Cavanna AE, Trimble MR. 2006. The precuneus: a review of its functional anatomy and behavioural correlates. Brain. 129:564–583.

Cavina-Pratesi C, Monaco S, Fattori P, Galletti C, McAdam TD, Quinlan DJ, Goodale MA, Culham JC. 2010. Functional magnetic resonance imaging reveals the neural substrates of arm transport and grip formation in reach-to-grasp actions in humans. J Neurosci. 30:10306–10323.

Chen Y, Monaco S, Byrne P, Yan X, Henriques DYP, Crawford JD. 2014. Allocentric versus egocentric representation of remembered reach targets in human cortex. J Neurosci. 34:12515–12526.

Cisek P, Kalaska JF. 2010. Neural mechanisms for interacting with a world full of action choices. Annu Rev Neurosci. 33:269–298.

Cisek P, Kalaska JF. 2002. Simultaneous encoding of multiple potential reach directions in dorsal premotor cortex. J Neurophysiol. 87:1149–1154.

Cisek P, Kalaska JF. 2005. Neural correlates of reaching decisions in dorsal premotor cortex: specification of multiple direction choices and final selection of action. Neuron. 45:801–814.

Connolly JD, Andersen RA, Goodale MA. 2003. FMRI evidence for a “parietal reach region” in the human brain. Exp brain Res. 153:140–145.

Connolly JD, Goodale MA, Cant JS, Munoz DP. 2007. Effector-specific fields for motor preparation in the human frontal cortex. Neuroimage. 34:1209–1219.

Connolly JD, Goodale MA, DeSouza JF, Menon RS, Vilis T. 2000. A comparison of frontoparietal fMRI activation during anti-saccades and anti-pointing. J Neurophysiol. 84:1645–1655.

Courtney SM, Ungerleider LG, Keil K, Haxby J V.1996. Object and spatial visual working memory activate separate neural systems in human cortex. Cereb Cortex. 6:39–49.

Culham JC, Cavina-Pratesi C, Singhal A. 2006. The role of parietal cortex in visuomotor control: what have we learned from neuroimaging? Neuropsychologia. 44:2668–2684.

Curtis CE, Connolly JD. 2008. Saccade preparation signals in the human frontal and parietal cortices. J Neurophysiol. 99(1):133-145.

Curtis CE, Rao VY, D'Esposito M. 2004. Maintenance of spatial and motor codes during oculomotor delayed response tasks. J Neurosci. 24(16):3944-3952.

Curtis CE. 2006. Prefrontal and parietal contributions to spatial working memory. Neuroscience 139(1):173-80.

DeSouza JF, Dukelow SP, Gati JS, Menon RS, Andersen RA, Vilis T. 2000. Eye position signal modulates a human parietal pointing region during memory-guided movements. J Neurosci. 20:5835–5840.

Engel SA, Glover GH, Wandell BA. 1997. Retinotopic organization in human visual cortex and the spatial precision of functional MRI. Cereb Cortex. 7:181–192.

Fabbri S, Caramazza A, Lingnau A. 2012. Distributed sensitivity for movement amplitude in directionally tuned neuronal populations. J Neurophysiol. 107:1845–1856.

Fernandez-Ruiz J, Goltz HC, DeSouza JFX, Vilis T, Crawford JD. 2007. Human parietal "reach region" primarily encodes intrinsic visual direction, not extrinsic movement direction, in a visual motor dissociation task. Cereb Cortex. 17:2283–2292.

Filimon F, Nelson JD, Huang R-S, Sereno MI. 2009. Multiple parietal reach regions in humans: cortical representations for visual and proprioceptive feedback during on-line reaching. J Neurosci. 29:2961–2971.

Flanagan JR, Johansson RS. 2003. Action plans used in action observation. Nature. 424:769–771.

Gail A, Andersen RA. 2006. Neural dynamics in monkey parietal reach region reflect context-specific sensorimotor transformations. J Neurosci. 26:9376–9384.

Gail A, Klaes C, Westendorff S. 2009. Implementation of spatial transformation rules for goal-directed reaching via gain modulation in monkey parietal and premotor cortex. J Neurosci. 29(30):9490-9499.

Gallivan JP, Cavina-Pratesi C, Culham JC. 2009. Is that within reach? fMRI reveals that the human superior parieto-occipital cortex encodes objects reachable by the hand. J Neurosci. 29:4381–4391.

Gallivan JP, Culham JC. 2015. Neural coding within human brain areas involved in actions. Curr Opin Neurobiol. 33:141–149.

Gallivan JP, McLean A, Culham JC. 2011. Neuroimaging reveals enhanced activation in a reach-selective brain area for objects located within participants' typical hand workspaces. Neuropsychologia. 49:3710–3721.

Gertz H, Fiehler K. 2015. Human posterior parietal cortex encodes the movement goal in a pro-/anti-reach task. J Neurophysiol. 114:170–183.

Gutteling TP, Petridou N, Dumoulin SO, Harvey BM, Aarnoutse EJ, Kenemans JL, Neggers SF. 2015. Action preparation shapes processing in early visual cortex. 35(16):6472-6480.

Hawkins KM, Sayegh P, Yan X, Crawford JD, Sergio LE. 2013. Neural activity in superior parietal cortex during rule-based visual-motor transformations. J Cogn Neurosci. 25:436–454.

Henriques DY, Klier EM, Smith MA, Lowy D, Crawford JD. 1998. Gaze-centered remapping of remembered visual space in an open-loop pointing task. J Neurosci. 18:1583–1594.

Hirnstein M, Bayer U, Ellison A, Hausmann M. 2011. TMS over the left angular gyrus impairs the ability to discriminate left from right. Neuropsychologia. 49(1):29-33.

Jerde TA, Merriam EP, Riggall AC, Hedges JH, Curtis CE. 2012. Prioritized maps of space in human frontoparietal cortex. 32(48):17382-90.

Konen CS, Mruczek REB, Montoya JL, Kastner S. 2013. Functional organization of human posterior parietal cortex: grasping- and reaching-related activations relative to topographically organized cortex. J Neurophysiol. 109:2897–2908.

Kravitz DJ, Saleem KS, Baker CI, Mishkin M. 2011 A new neural framework for visuospatial processing. Nat Rev Neurosci. 12(4):217-230.

Kuang S, Morel P, Gail A. 2016. Planning Movements in Visual and Physical Space in Monkey Posterior Parietal Cortex. Cerebral Cortex. 26(2):731-747.

Macaluso E, Frith C, Driver J. 2000. Selective spatial attention in vision and touch: unimodal and multimodal mechanisms revealed by PET. J Neurophysiol. 83:3062–3075.

Makino Y, Yokosawa K, Takeda Y, Kumada T. 2004. Visual search and memory search engage extensive overlapping cerebral cortices: an fMRI study. Neuroimage. 23:525–533.

Malik P, Dessing JC, Crawford JD. 2015. Role of early visual cortex in trans-saccadic memory of object features. J Vis. 15(11):7.

Medendorp WP, Goltz HC, Crawford JD, Vilis T. 2005. Integration of target and effector information in human posterior parietal cortex for the planning of action. J Neurophysiol. 93:954–962.

Medendorp WP, Goltz HC, Vilis T. 2006. Directional selectivity of BOLD activity in human posterior parietal cortex for memory-guided double-step saccades. J Neurophysiol. 95:1645–1655.

Medendorp WP, Goltz HC, Vilis T, Crawford JD. 2003. Gaze-centered updating of visual space in human parietal cortex. J Neurosci. 23:6209–6214.

Messier J, Kalaska JF. 2000. Covariation of primate dorsal premotor cell activity with direction and amplitude during a memorized-delay reaching task. J Neurophysiol. 84(1):152-165.

Monaco S, Cavina-Pratesi C, Sedda A, Fattori P, Galletti C, Culham JC. 2011. Functional magnetic resonance adaptation reveals the involvement of the dorsomedial stream in hand orientation for grasping. J Neurophysiol. 106:2248–2263.

Olson CR. 2003. Brain representation of object-centered space in monkeys and humans. Annu Rev Neurosci. 26:331–354.

Pasternak T, Greenlee MW. 2005. Working memory in primate sensory systems. Nat Rev Neurosci. 6:97–107.

Perenin MT, Vighetto A. 1988. Optic ataxia: a specific disruption in visuomotor mechanisms. I. Different aspects of the deficit in reaching for objects. Brain. 111 (Pt 3:643–674.

Picard N, Strick PL. 2001. Imaging the premotor areas. Curr Opin Neurobiol. 11:663–672.

Prado J, Clavagnier S, Otzenberger H, Scheiber C, Kennedy H, Perenin M-T. 2005. Two cortical systems for reaching in central and peripheral vision. Neuron. 48:849–858.

Pratte MS, Tong F. 2014. Spatial specificity of working memory representations in the early visual cortex. J Vis. 14(3):22.

Rawley JB, Constantinidis C. 2009. Neural correlates of learning and working memory in the primate posterior parietal cortex. Neurobiol Learn Mem. 91:129–138.

Reed CL, Grubb JD, Steele C. 2006. Hands up: attentional prioritization of space near the hand. J Exp Psychol Hum Percept Perform. 32:166–177.

Rossetti Y, Pisella L, Vighetto A. 2003. Optic ataxia revisited: visually guided action versus immediate visuomotor control. Exp Brain Res. 153(2):171-179.

Sadeh M, Sajad A, Wang H, Yan X, Crawford JD. 2015. Spatial transformations between superior colliculus visual and motor response fields during head-unrestrained gaze shifts. Eur J Neurosci. 42(11):2934-51.

Sajad A, Sadeh M, Keith GP, Yan X, Wang H, Crawford JD. 2015. Visual-Motor Transformations Within Frontal Eye Fields During Head-Unrestrained Gaze Shifts in the Monkey. Cereb Cortex. 25(10):3932-52.

Singh KD, Smith AT, Greenlee MW. 2000. Spatiotemporal frequency and direction sensitivities of human visual areas measured using fMRI. Neuroimage. 12:550–564.

Singhal A, Monaco S, Kaufman LD, Culham JC. 2013. Human fMRI reveals that delayed action re-recruits visual perception. PLoS One. 8(9):e73629.

Srimal R, Curtis CE. 2008. Persistent neural activity during the maintenance of spatial position in working memory. Neuroimage. 39(1):455-468.

Tosoni A, Galati G, Romani GL, Corbetta M. 2008. Sensory-motor mechanisms in human parietal cortex underlie arbitrary visual decisions. Nat Neurosci. 11:1446–1453.

Uchimura, M., Nakano, T., Morito, Y., Ando, H., & Kitazawa, S. (2015). Automatic representation of a visual stimulus relative to a background in the right precuneus. Eur J Neurosci, 42(1), 1651-1659.

Van Der Werf J, Jensen O, Fries P, Medendorp WP. 2008. Gamma-band activity in human posterior parietal cortex encodes the motor goal during delayed prosaccades and antisaccades. J Neurosci. 28(34):8397-8405.

Van Der Werf J, Jensen O, Fries P, Medendorp WP. 2010. Neuronal synchronization in human posterior parietal cortex during reach planning. J Neurosci. 30(4):1402-1412.

Vesia M, Crawford JD. 2012. Specialization of reach function in human posterior parietal cortex. Exp brain Res. 221:1–18.

Vesia M, Monteon JA, Sergio LE, Crawford JD. 2006. Hemispheric asymmetry in memory-guided pointing during single-pulse transcranial magnetic stimulation of human parietal cortex. J Neurophysiol. 96(6):3016-3027.

Vesia M, Prime SL, Yan X, Sergio LE, Crawford JD. 2010. Specificity of human parietal saccade and reach regions during transcranial magnetic stimulation. J Neurosci. 30:13053–13065.

Weinrich M, Wise SP. 1982. The premotor cortex of the monkey. J Neurosci. 2(9):1329-1345.

Westendorff S, Klaes C, Gail A. 2010. The cortical timeline for deciding on reach motor goals. J Neurosci. 30:5426–5436.

Zhang M, Barash S. 2000. Neuronal switching of sensorimotor transformations for antisaccades. Nature. 408(6815):971-975.

Figure 1

A)

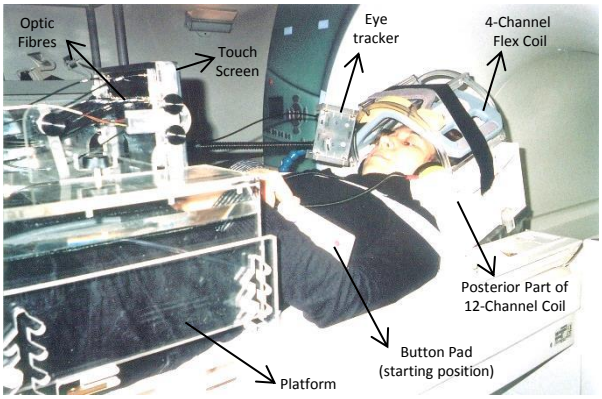
Optic Fibres
Touch Screen
Eye tracker
4-Channel Flex Coil
Posterior Part of 12-Channel Coil
Button Pad (starting position)
Platform

B)

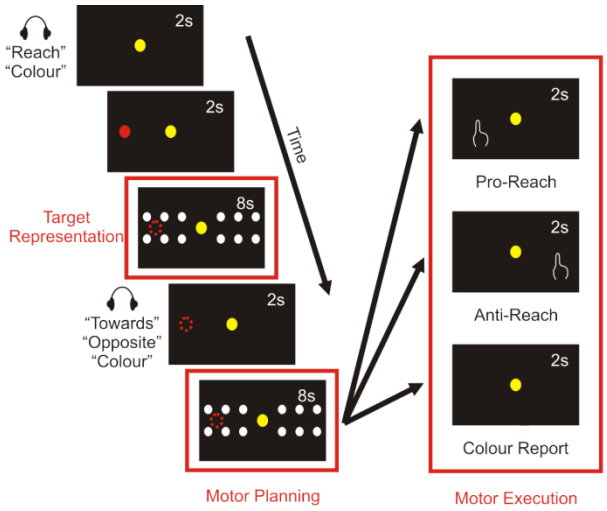
"Reach" "Colour"
2s
2s
Time
Target Representation
8s
"Towards" "Opposite" "Colour"
2s
8s
Motor Planning
2s
Pro-Reach
2s
Anti-Reach
2s
Colour Report
Motor Execution

Figure 2

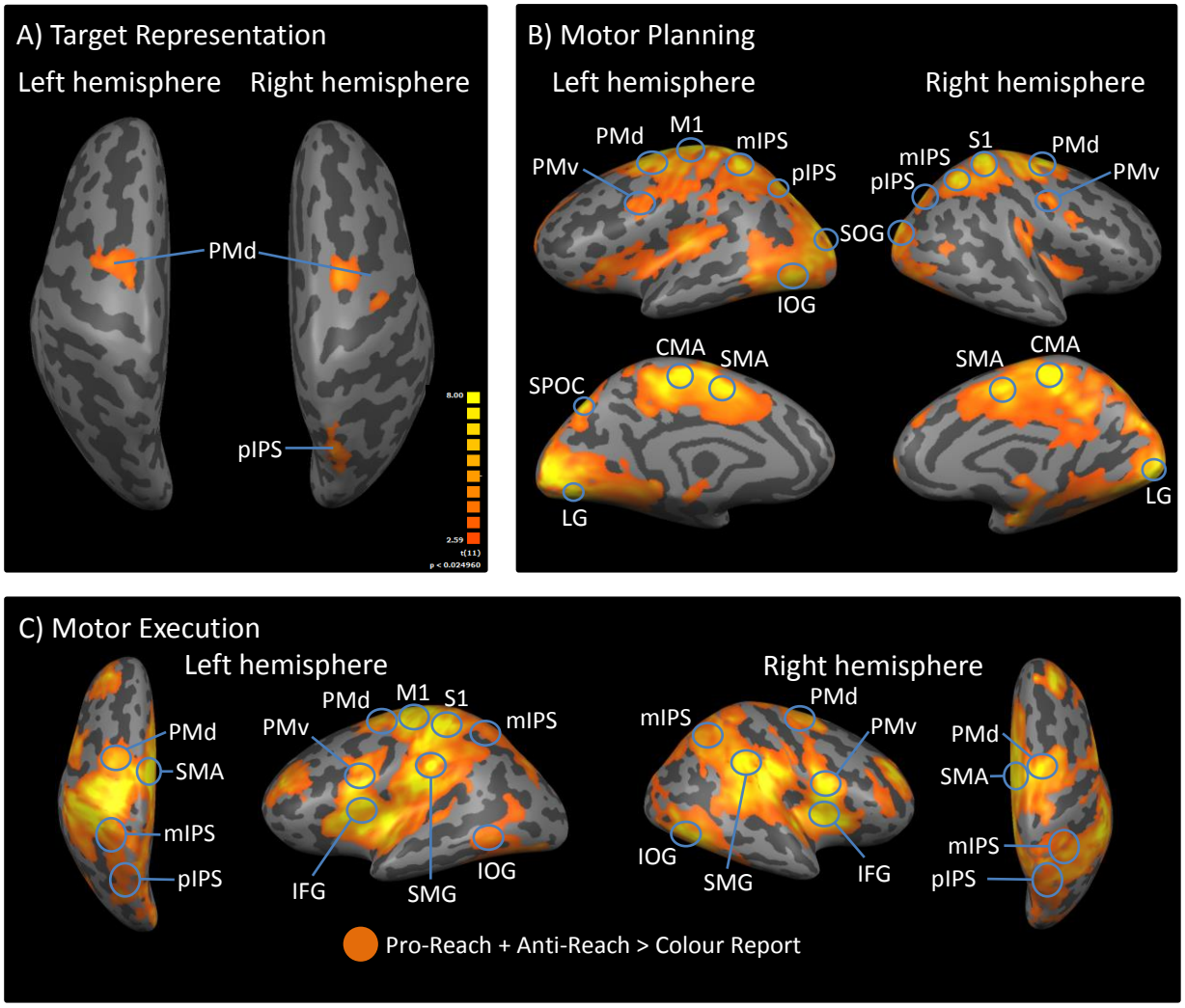
A) Target Representation
Left hemisphere
Right hemisphere
PMd
pIPS
8.00
2.59
t(11)
p < 0.024960
B) Motor Planning
Left hemisphere
Right hemisphere
PMd
M1
mIPS
PMv
pIPS
SOG
IOG
S1
CMA
SMA
SPOC
LG
C) Motor Execution
Left hemisphere
Right hemisphere
PMd
SMA
mIPS
pIPS
PMv
M1
S1
IFG
SMG
IOG
Pro-Reach + Anti-Reach > Colour Report

Figure 3

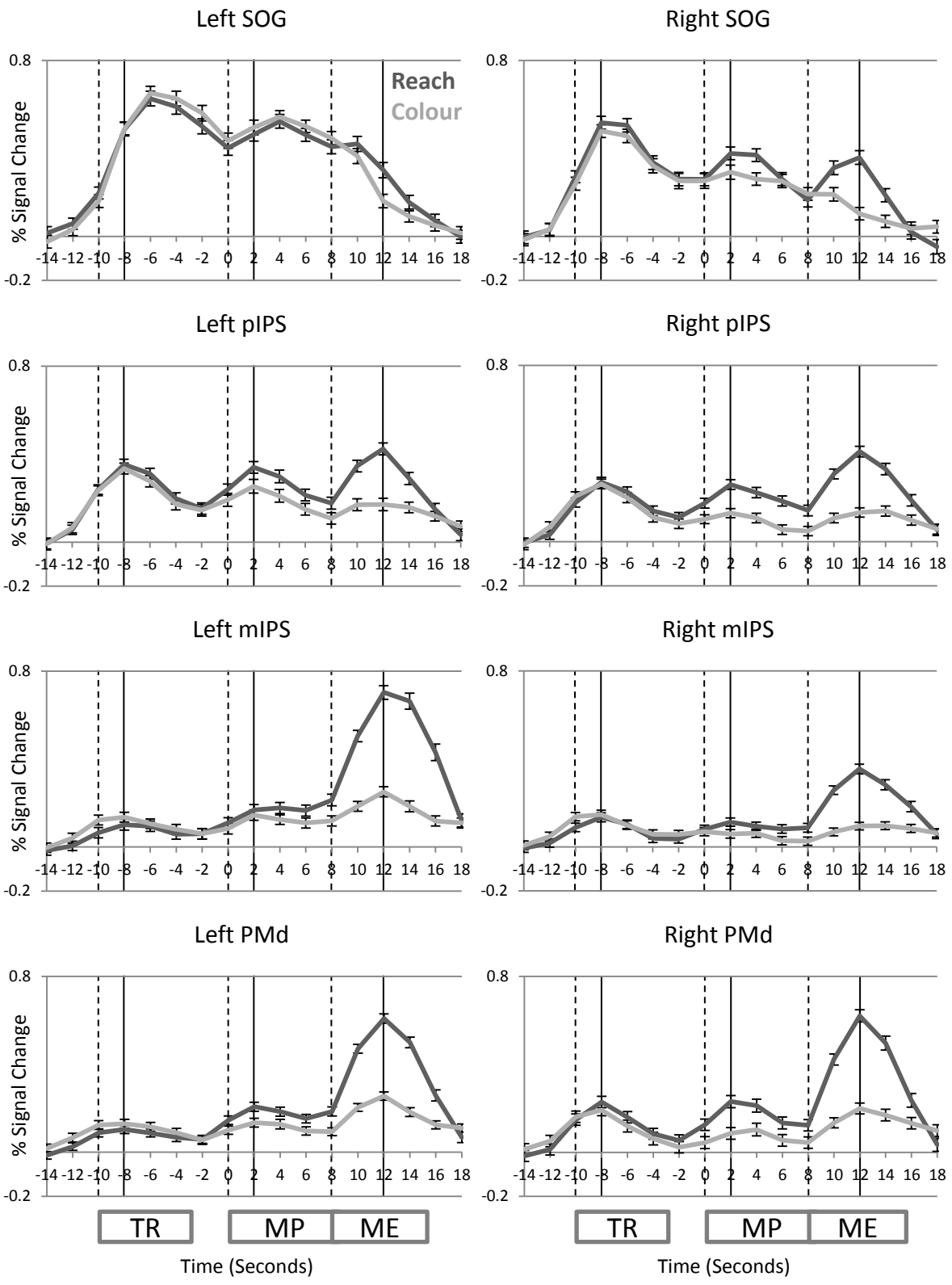
Left SOG
Right SOG
Left pIPS
Right pIPS
Left mIPS
Right mIPS
Left PMd
Right PMd
Reach
Colour
% Signal Change
0.8
-0.2
-14 -12 -10 -8 -6 -4 -2 0 2 4 6 8 10 12 14 16 18
TR
MP
ME
Time (Seconds)

Figure 4

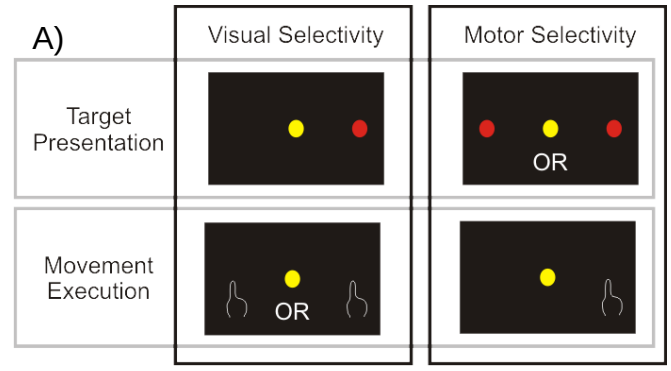
A)
Visual Selectivity
Motor Selectivity
Target Presentation
OR
Movement Execution
OR

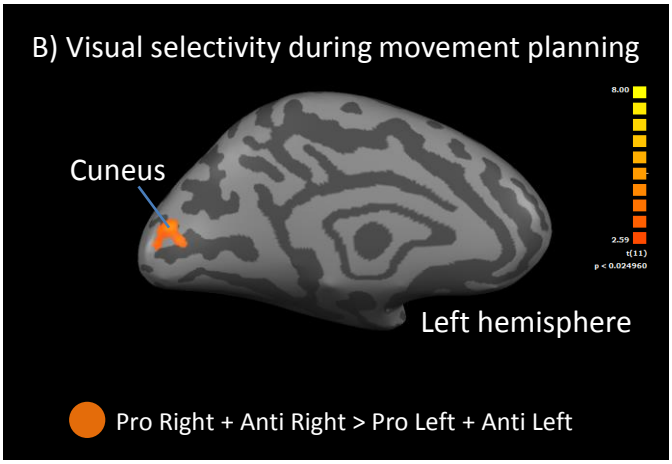
B) Visual selectivity during movement planning
Cuneus
8.00
2.59
t(11)
p < 0.024960
Left hemisphere
Pro Right + Anti Right > Pro Left + Anti Left

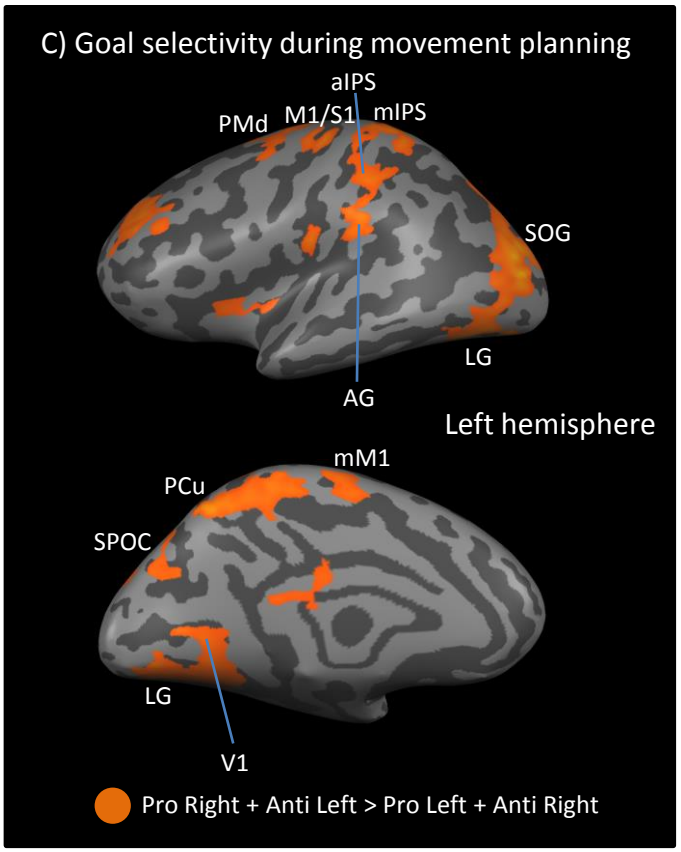
C) Goal selectivity during movement planning
aIPS
PMd
M1/S1
mIPS
SOG
LG
AG
Left hemisphere
mM1
PCu
SPOC
LG
V1
Pro Right + Anti Left > Pro Left + Anti Right

Figure 5

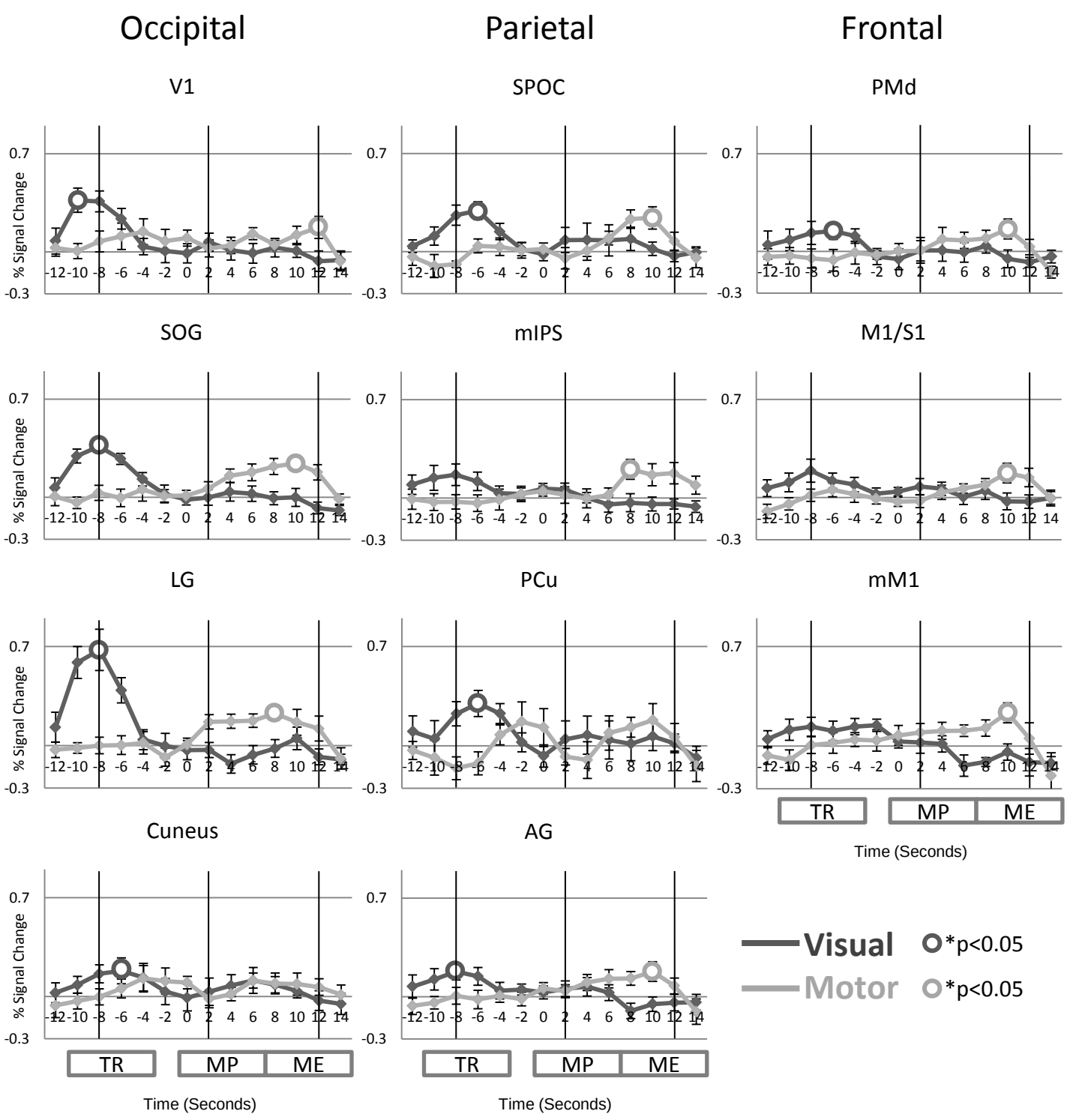
Occipital
Parietal
Frontal
V1
SPOC
PMd
SOG
mIPS
M1/S1
LG
PCu
mM1
Cuneus
AG
% Signal Change
0.7
-0.3
-12 -10 -8 -6 -4 -2 0 2 4 6 8 10 12 14
TR
MP
ME
Time (Seconds)
Visual
*p<0.05
Motor
*p<0.05

Figure 6

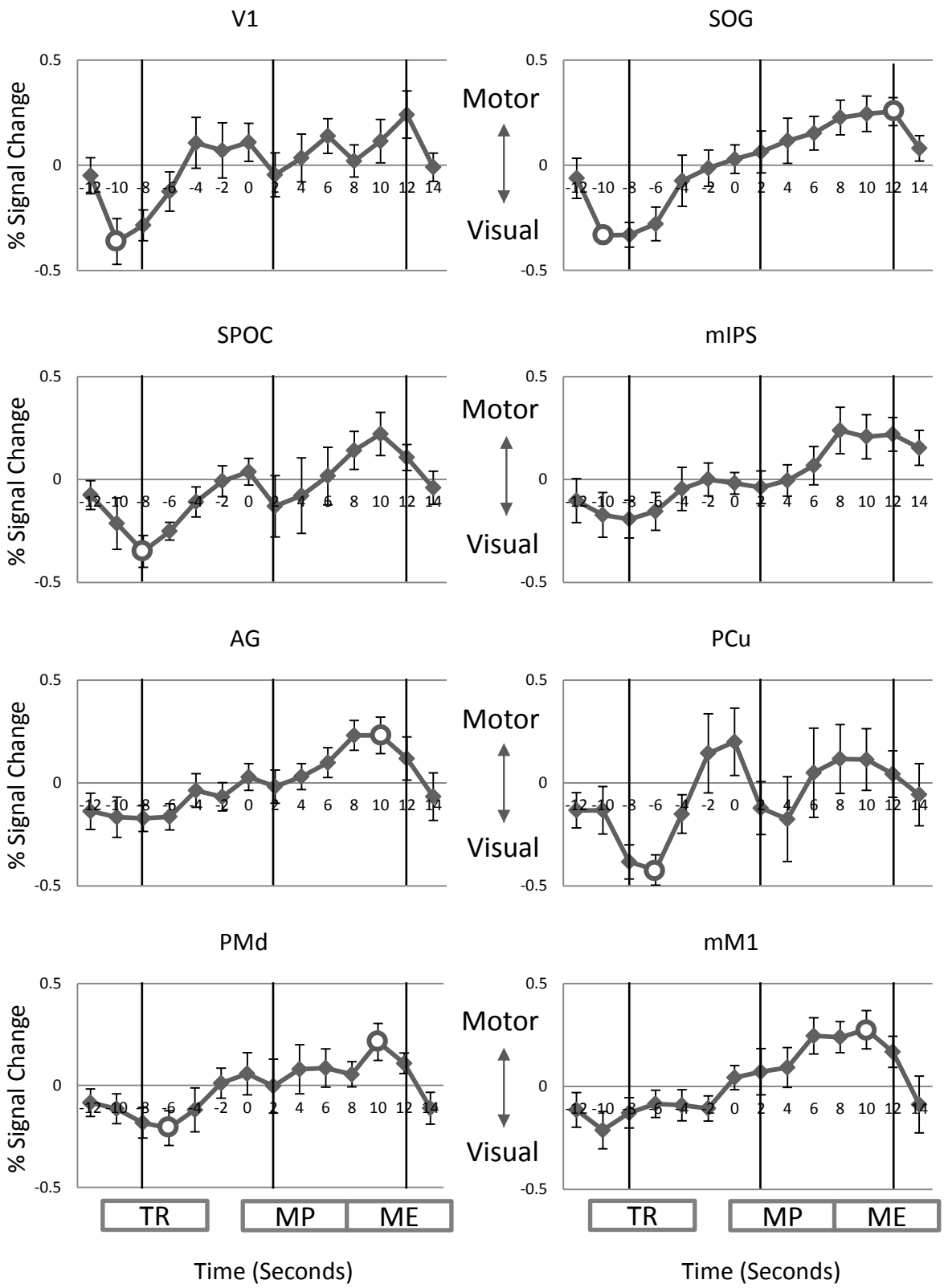
V1
SOG
SPOC
mIPS
AG
PCu
PMd
mM1
% Signal Change
0.5
0
-0.5
Motor
Visual
-12 -10 -8 -6 -4 -2 0 2 4 6 8 10 12 14
TR
MP
ME
Time (Seconds)

Figure 7

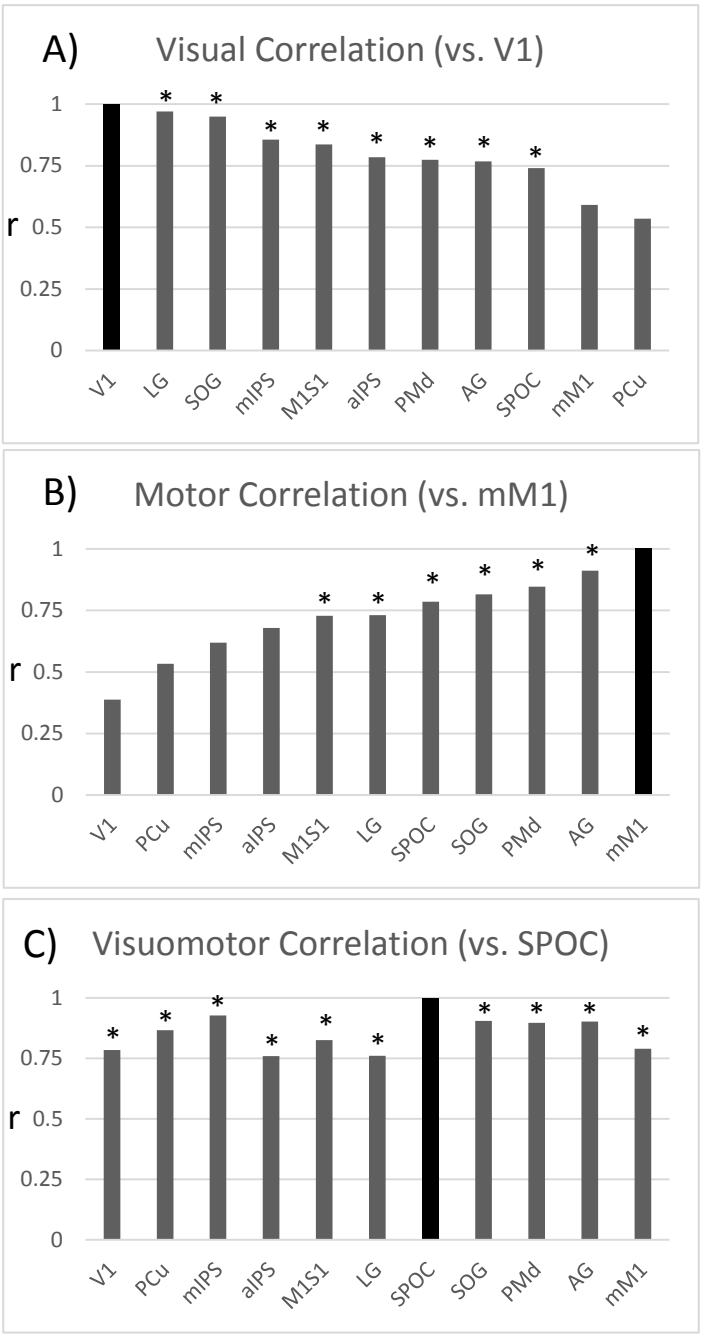
A)
Visual Correlation (vs. V1)
r
1
0.75
0.5
0.25
0
V1
LG
SOG
mIPS
M1S1
aIPS
PMd
AG
SPOC
mM1
PCu
B)
Motor Correlation (vs. mM1)
V1
PCu
mIPS
aIPS
M1S1
LG
SPOC
SOG
PMd
AG
mM1
C)
Visuomotor Correlation (vs. SPOC)
V1
PCu
mIPS
aIPS
M1S1
LG
SPOC
SOG
PMd
AG
mM1

Figure 8

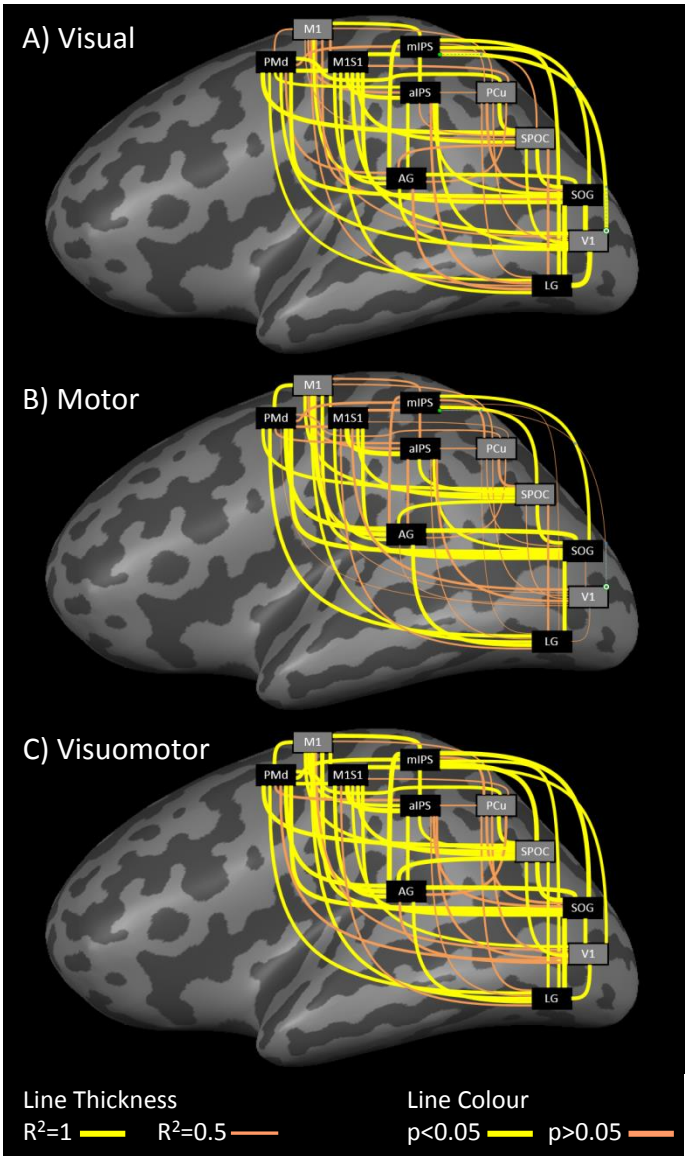
A) Visual
M1
PMd
M1S1
mIPS
aIPS
PCu
SPOC
AG
SOG
V1
LG
B) Motor
M1
PMd
M1S1
mIPS
aIPS
PCu
SPOC
AG
SOG
V1
LG
C) Visuomotor
M1
PMd
M1S1
mIPS
aIPS
PCu
SPOC
AG
SOG
V1
LG
Line Thickness
R2=1
R2=0.5
Line Colour
p<0.05
p>0.05

Supplementary figure 1

A) Target Representation

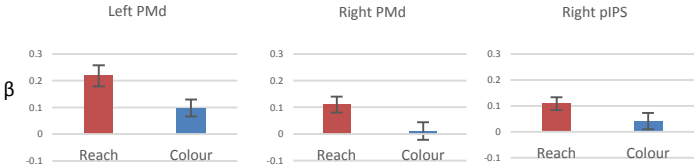

B) Movement Planning

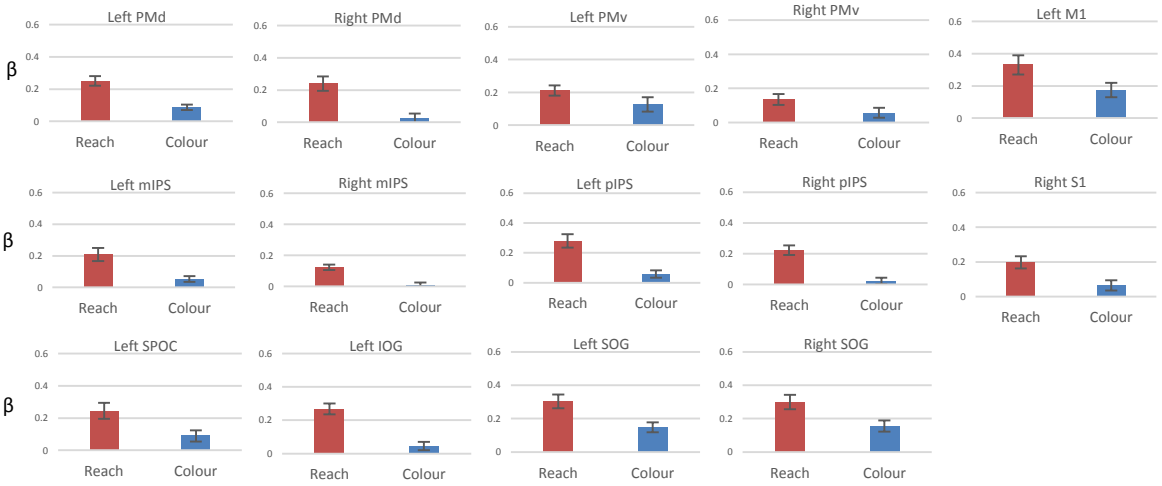

C) Movement Execution

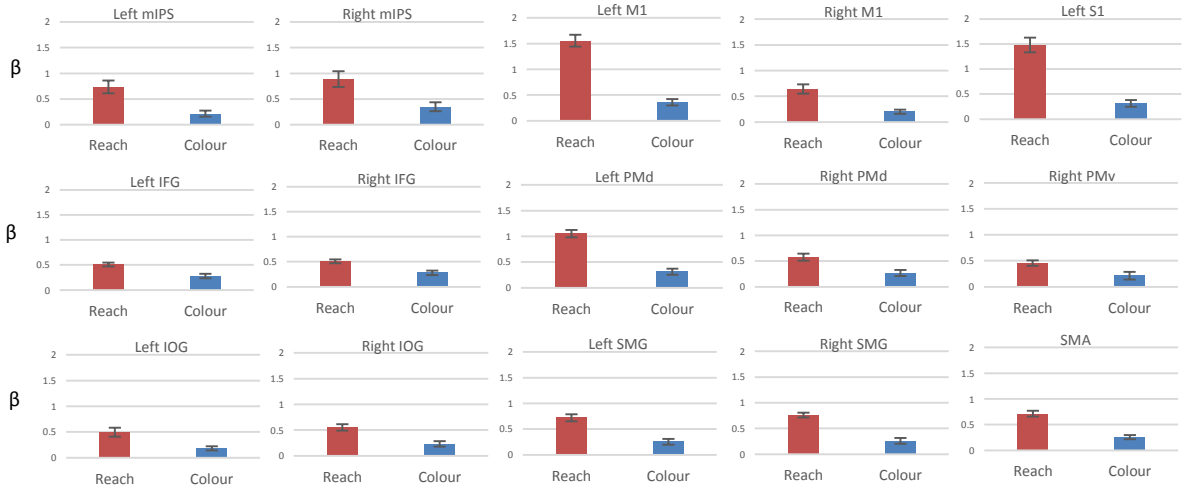

Supplementary Figure 2

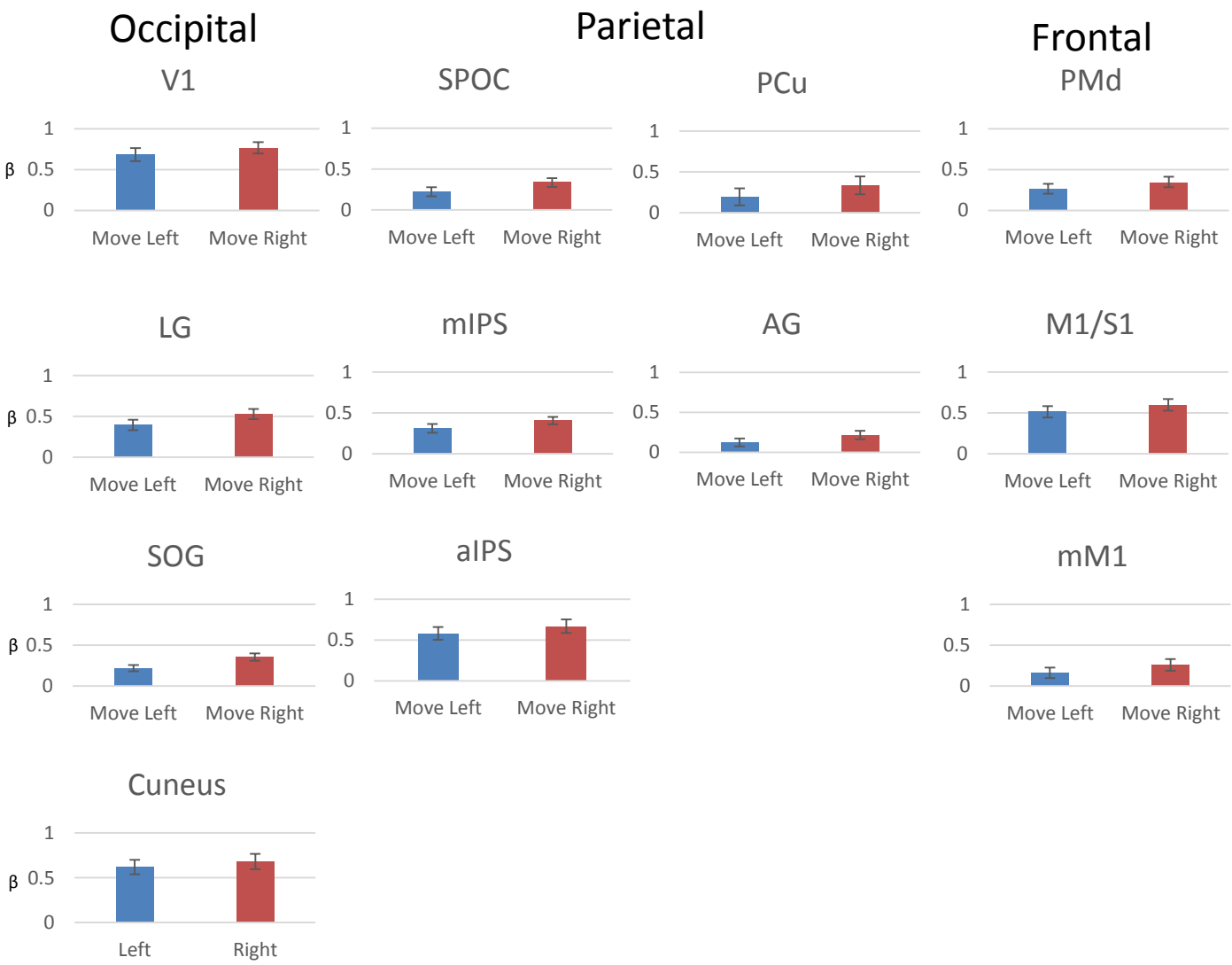

Supplementary Figure 3

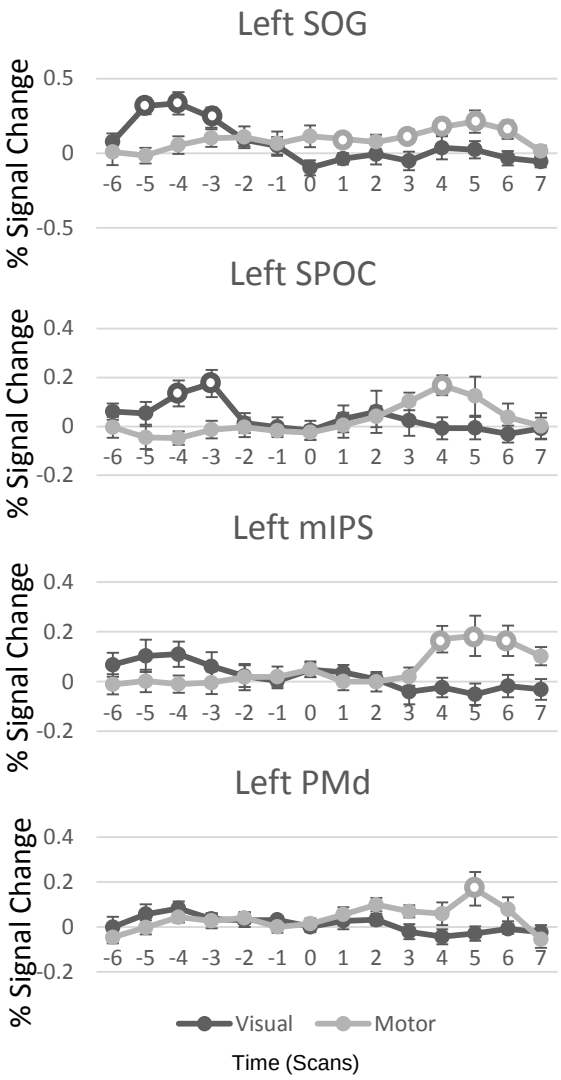

Supplementary Figure 4

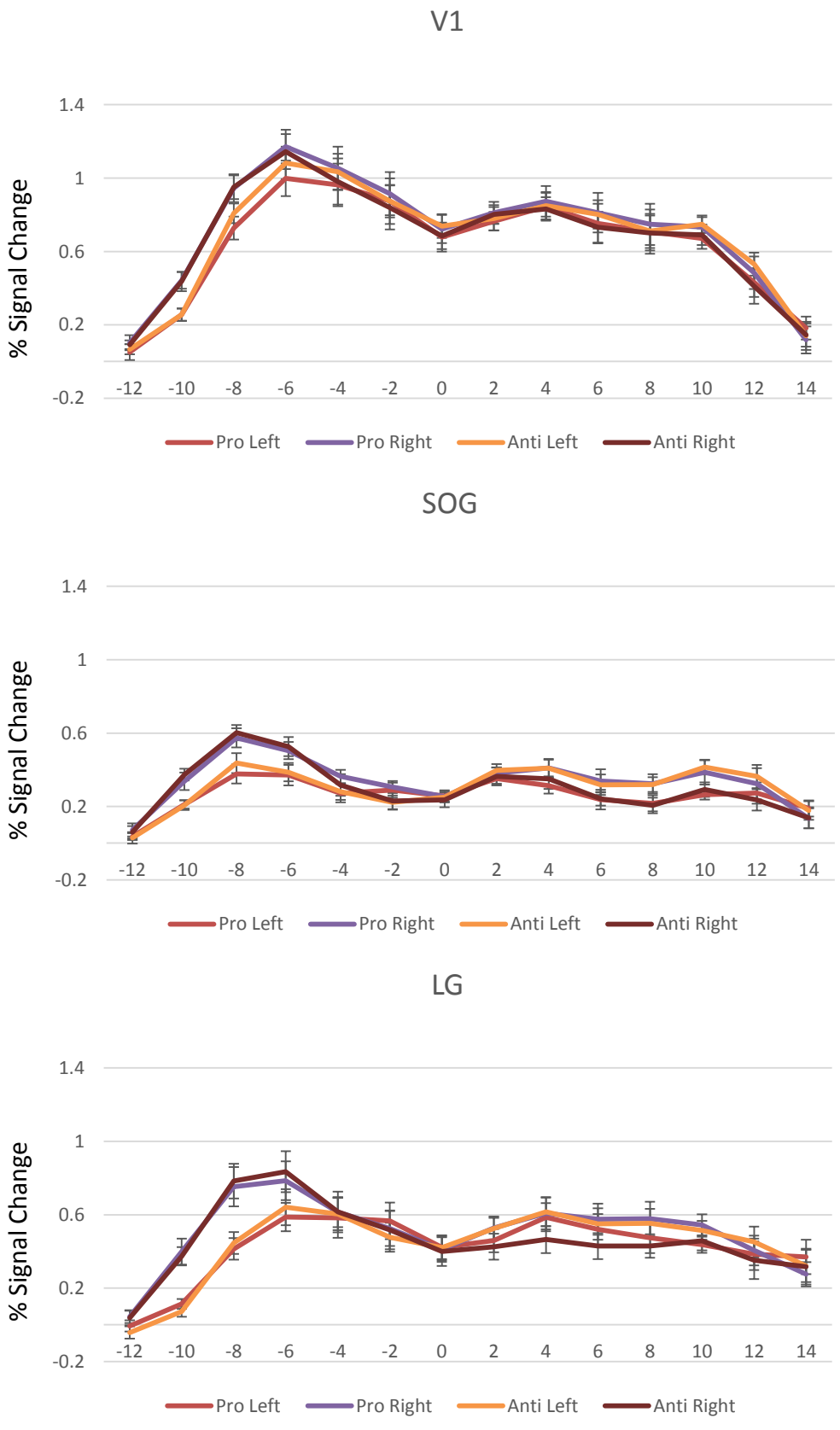

Supplementary Figure 5

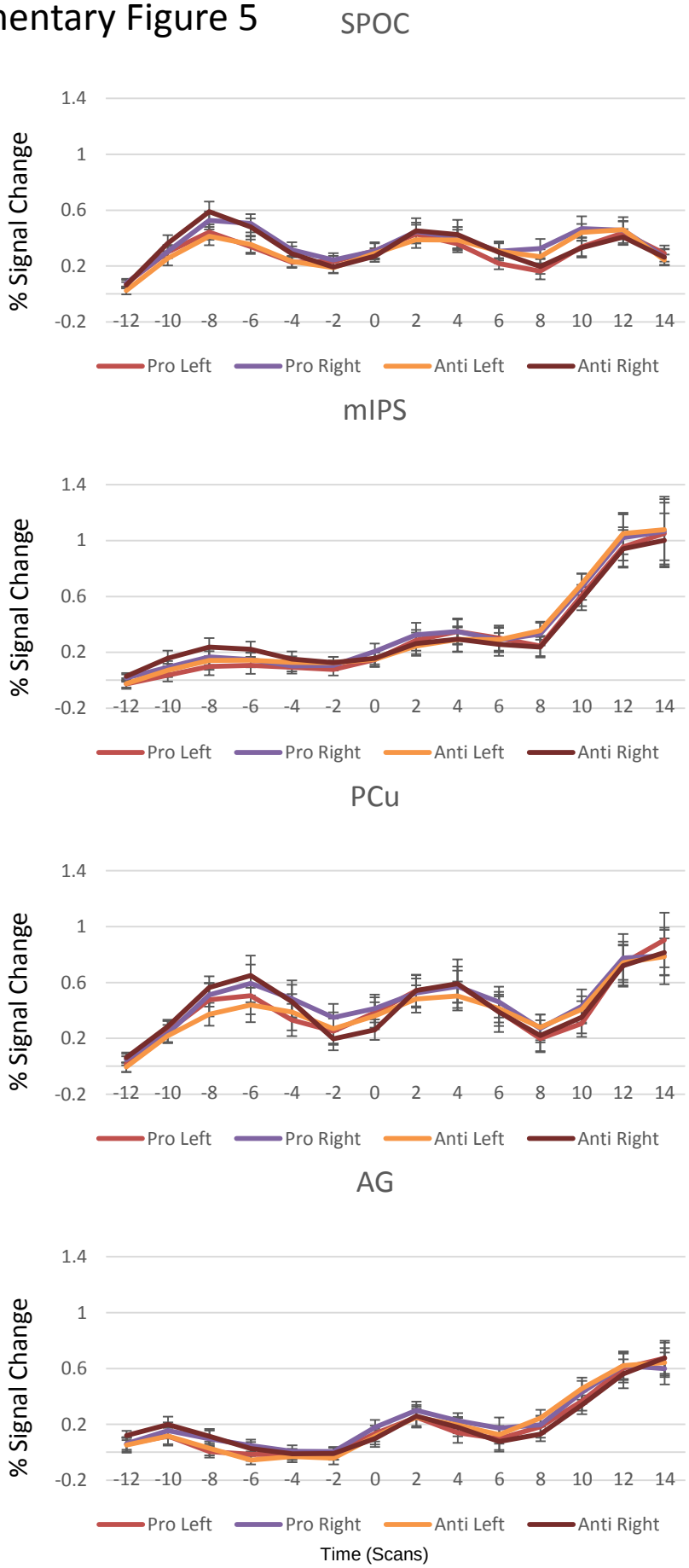

Supplementary Figure 6

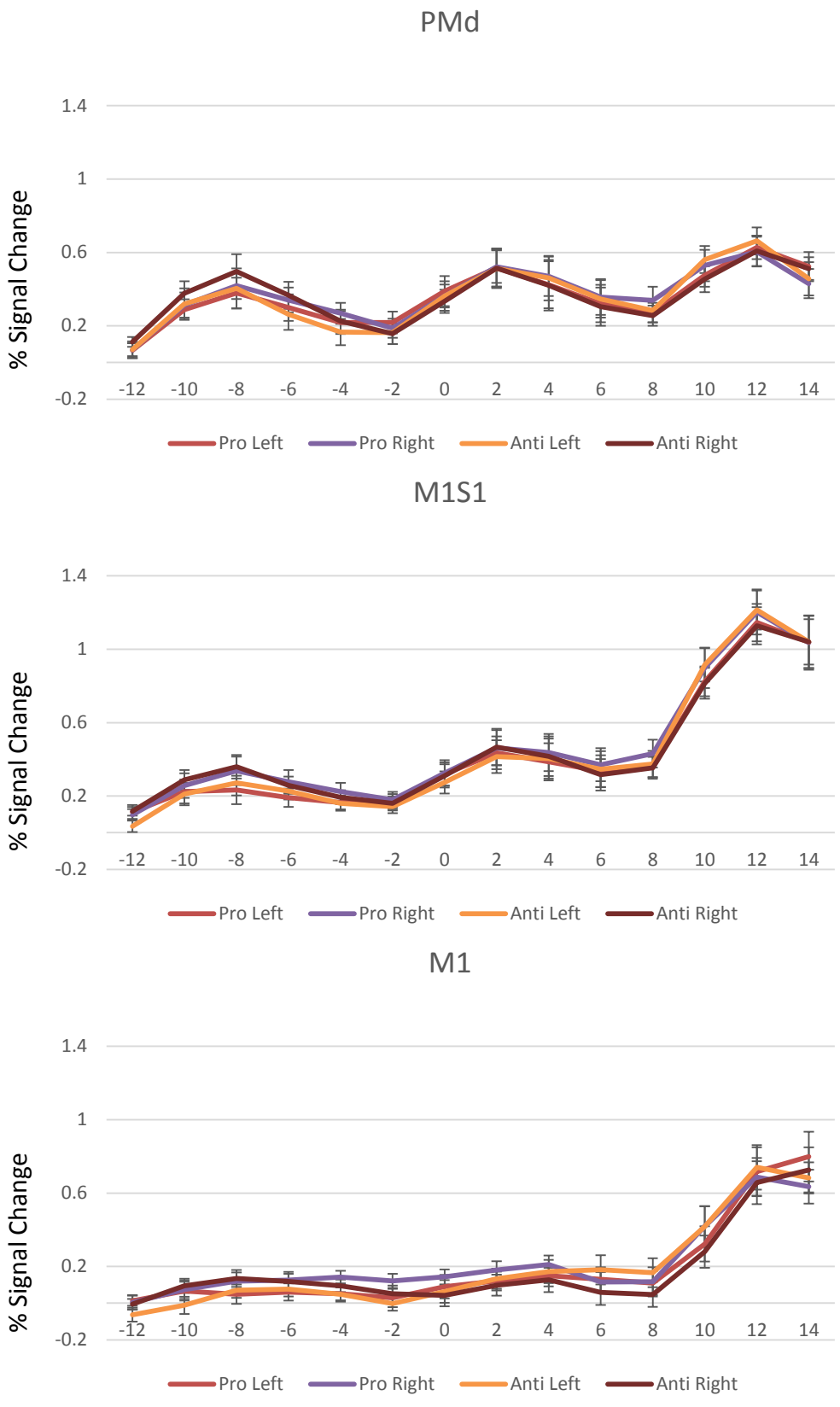

Supplementary Figure 7

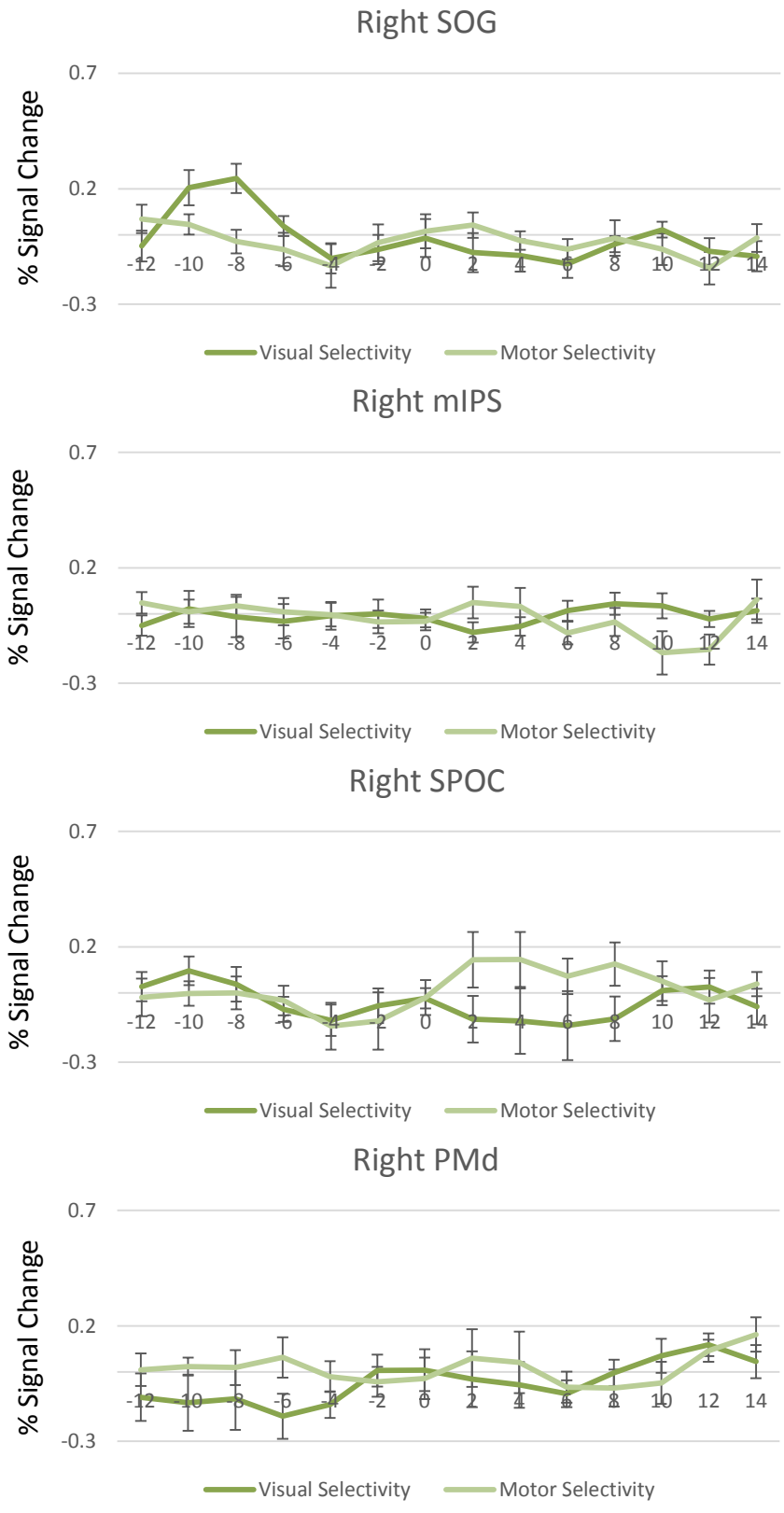

Supplementary Figure 8